A Database of Aircraft Measurements of Carbon Monoxide (CO) with High Temporal and Spatial Resolution during 2011 – 2021

Chaoyang Xue[1], Gisèle Krysztofiak[1], Vanessa Brocchi[1], Stéphane Chevrier[1], Michel Chartier[1], Patrick Jacquet[1], Claude Robert[1], Valéry Catoire[1]*

[1]Laboratoire de Physique et Chimie de l'Environnement et de l'Espace (LPC2E), CNRS – Université Orléans – CNES (UMR 7328), 45071 Orléans cedex 2, France

Correspondence: Valéry Catoire (valery.catoire@cnrs-orleans.fr)

Abstract

To understand tropospheric air pollution at regional and global scales, the SPIRIT airborne instrument (SPectromètre Infra-Rouge In situ Toute altitude) was developed and used on aircraft to measure volume mixing ratios of carbon monoxide (CO), an important indicator of air pollution, during the last decade. SPIRIT could provide high-quality CO measurements with 1σ precision of 0.3 ppbv at a time resolution of 1.6 s thanks to the coupling of a quantum cascade laser to a Robert optical multi-pass cell. It can be operated on different aircraft such as Falcon-20 and ATR-42 from DLR (Germany) and SAFIRE (CNRS-CNES-Météo France). With support from various projects, more than 200 flight hours measurements were conducted over three continents (Europe, Asia, and Africa), including two inter-continental ~~measurements~~ transects (Europe-Asia and Europe-Africa). Levels of CO and its ~~horizontal~~ spatial ~~and vertical~~ distribution are briefly discussed and compared between different regions/continents. CO generally decreases with altitude except ~~for the measurements in high-latitude regions~~in some cases, indicating the important contribution of long-distance transport to CO levels ~~at high-latitude regions~~. A 3D trajectory mapped by CO level was plotted for each flight and is presented in this study (including a supplementary information). The database is archived on ~~the~~ AERIS database (https://doi.org/10.25326/440), the French national center for atmospheric observations (Catoire et al., 2023). Besides, it could help to validate model performances and satellite measurements. For instance, the database covers measurements at high-latitude regions (i.e., Kiruna, Sweden, 68˚N) where satellite measurements are still challengeable and at low-latitude regions (West Africa and South-East Asia) where in situ data are scarce and satellites need more validation by airborne measurements.

1 Introduction

The study of atmospheric composition has been widely conducted and understood through comprehensive field campaigns and ground level air quality monitoring networks ~~at the ground level~~ (including mountain summit- and tower- based platforms) in the world (e.g., Acharja et al., 2020; Andreae et al., 2015; Brown et al., 2013; Daellenbach et al., 2020; David et al., 2021; Guo et al., 2014; Hanke et al., 2003; Harrison et al., 2012; Ravi Kant Pathak et al., 2009; Ryerson et al., 2013; Sellers et al., 1995; Shi et al., 2019; Tang et al., 2021). The very recent fifth WHO Air Quality Database (https://www.who.int/data/gho/data/themes/air-pollution/who-air-quality-database, last access: ~~18 February~~July 18, 2023) compiles ground measurements on air quality for over 6000 cities/human settlements in more than 100 countries. This provides a large body of datasets to understand air quality, its health impacts, and atmospheric chemistry/dynamics in the lower atmosphere as well as its interaction with the biosphere, and to assess model performance in predicting near-ground atmospheric composition. However, those measurements are typically limited to the boundary layer, arising challenges and limitations in understanding ~~regional or global atmospheric processes including~~ atmospheric chemistry and dynamics ~~since the latter extend well above the surface~~above this~~e boundary~~ layer (i.e., free troposphere, stratosphere)~~,~~ and~~indicat~~ showing the necessity of airborne measurements. Airborne measurements are also necessary for the validation of satellite observations which have undergone fast development and shown important prospects in the past decades. However, measurements at high-latitude regions are still challengeable for satellite, and hence, validation of satellite in those regions are of significant necessity (Hegarty et al., 2022; Wizenberg et al., 2021). Moreover, many important gases ~~are important~~ for atmospheric chemistry, air quality, and global climate have ~~but with~~ too low~~ an~~ abundance to be detected by satellite. The vertical profile and regional distribution of those species must be detected by in-situ airborne measurements.

Aircraft serving as a research platforms start~~s~~ in the late 1920's, beginning with meteorological measurements such as temperature and altitude in the UK (Gratton, 2012 and therein). Since the 1940's, scientists have been using aircraft to sample ~~the~~ air to better understand the composition and related processes of the atmosphere far above the surface (https://earthobservatory.nasa.gov/blogs/fromthefield/2016/07/26/long-history-of-using-aircraft-to-understand-the-atmosphere/, last access: ~~18 February~~July 18, 2023). Owning to the development of rapid-response and high-precision instruments, aircraft measurements beca~~o~~me more and more popular, particularly in North America and Europe (Ryerson et al., 2013; Fast et al., 2007; Hamburger et al., 2011; Fehsenfeld et al., 2006; Mallet et al., 2016; Andrés Hernández et al., 2021; Machado et al., 2018; Crawford et al., 2021). In addition to measurements within the boundary layer, ~~the~~ aircraft platforms could allow measurements through the troposphere and even ~~reach~~ the lower stratosphere (< 20 km above sea level (asl)), through which understanding the atmospheric dynamics and the distribution of pollution at both horizontal and vertical scales could be achieved.

Carbon monoxide (CO) is ~~the second largest~~an important atmospheric carbon compound~~ (after CO_2)~~, mainly emitted by incomplete combustion processes, e.g., biomass burning, fossil fuel combustion, etc. Its moderate lifetime of ca. 1-2 months indicates that its abundance is generally impacted by emissions at a regional scale. In ~~a~~ polluted atmospheres such as urban areas, CO is mainly produced from incomplete combustion processes such as coal/gasoline/diesel/biomass combustion, and its concentration could reach levels of several ppmv (Xue et al., 2020; Dekker et al., 2019). In the background atmosphere (e.g., remote areas, marine boundary layer) or the upper troposphere, CO is generally low (< 100 ppbv) (Lelieveld et al., 2008) mainly resulting from atmospheric oxidization processes e.g., the oxidation of methane by OH radicals. A high level of CO in a background atmosphere typically indicates impacts of regional transport (or convection/eruption for the upper troposphere) (Krysztofiak et al., 2018). Therefore, aircraft CO measurements can provide an overview of the pollution in the ~~target~~ studied region and are a good indicator of regional pollution levels and intensive emission events, e.g., wildfires (Jaffe and Wigder, 2012; Jaffe et al., 2022). There are already available aircraft CO measurements, which provide a broader spatial distribution. Those are mainly from US projects, such as TRACE-P in 2001 (Palmer et al., 2003), INTEX-B in 2006 (Luo et al., 2007), GoAmazon2014/5 in Brazil (Machado et al., 2018), WE-CAN in 2018 (Permar et al., 2021), and FIREX-AQ in 2019 (Bourgeois et al., 2022), and European projects, such as DABEX in 2006 (Johnson et al., 2008), EUCAARI-LONGREX and APPRAISE-ADIENT in 2008 (McMeeking et al., 2010), CLARIFY in 2017 (Haywood et al., 2021), EMeRGe-EU in 2017 and EMeRGe-Asia in 2018 (Forster et al., 2023), BLUESKY in 2020 (Voigt et al., 2022).

Another important utilization of aircraft measurements is the validation of chemical-transport model simulations. Satellite observations are more and more popularly used to study atmospheric composition. Many satellites can detect CO, such as MOPITT (https://terra.nasa.gov/about/terra-instruments/mopitt, last access: ~~18 February~~July 18, 2023), IASI (https://www.eumetsat.int/iasi, last access: ~~18~~ July 18, ~~February~~ 2023) and TROPOMI (http://www.tropomi.eu/, last access: ~~18 February~~July 18, 2023). However, satellite observations of CO need to be validated by measurement at different regions. For instance, recently, Wizenberg et al. (2021) compared CO measurements from TROPOMI, the Atmospheric Chemistry Experiment (ACE) Fourier transform spectrometer (FTS), and a high-Arctic ground-based FTS. They found different biases in different regions, e.g., positive biases (ca. +7%) in northern and southern polar regions and negative biases (ca. -9%) in equatorial regions.

Herein, based on a sensitive airborne instrument (SPIRIT) with high-resolution and high-precision CO detection, seven aircraft campaigns funded by European and French national projects were conducted worldwide between 2011 and 2021, accompanied by two inter-continental measurements. This ~~database~~ paper summarizes all the data obtained during those aircraft campaigns.

2 Method: the SPIRIT Instrument

2.1 Set-up

In 2011, an infrared laser absorption spectrometer called SPIRIT (SPectromètre Infra-Rouge In situ Toute altitude) was developed at LPC2E for airborne measurements of trace gases in the troposphere. Details about this instrument can be found in Catoire et al (2017). Briefly, the coupling of a single Robert multi-pass optical cell (with a path length to be adjusted up to

167.78 m) with three interchangeable quantum cascade lasers (QCLs) was designed, which allows selecting trace gases to measure, according to the scientific objectives. Absorptions of the laser radiations by the species in the cell at reduced pressure (<40 h Pa) are quantified using a HgCdTe photodetector cooled by the Stirling cycle, according to the Beer-lambert law. For CO, two absorption rovibrational lines were successively used, namely 2179.772 and 2183.224 cm^{-1}, with the functioning conditions for the lasers indicated in Table 1~~Table 1~~. CO was ~~always~~ measured ~~for~~ on all the scientific flights, regarding its essential role in atmospheric chemistry, as discussed in Section 1. Hence, in this database, all the airborne CO measurements during the last decade are summarized.

Table 1: Parameters/performance of the SPIRIT instrument.

Years of Meas.	Spectral domain swept (cm^{-1})	Current + ramp (mA)	T_QCL (ºC)	Precision (1σ, ppbv)
2011-2016	2179.70-2179.85	600 + 13	-12.5	0.3
2019-2021	2183.15-2183.35	595 + 15	-13.2	0.3

2.2 QA/QC (Quality Assurance / Quality Control)

In Catoire et al (2017), laboratory experiments and in-flight intercomparisons with other instruments were conducted to assess the performances of SPIRIT and the quality of the data. Besides, for each field campaign, in-flight calibrations were~~as~~ also conducted during every flight. It was noted that until 2016 (see Section 3.5), SPIRIT could provide high-quality CO data with a precision of 0.3 ppbv (1σ) and an overall uncertainty of less than 1 ppbv, when ~~we perform~~ regular in-flight calibration vs. WMO standard were performed. This is still the case since 2016. As an example, in Section 3.7, we present data with in-flight calibrations.

3 Results and Discussion

During the 2011-2021 period, SPIRIT was used in 7 aircraft campaigns with 74 scientific flights. In total, 208.8 hours of in-flight CO measurements were obtained (

Table 2~~Table 2~~). Figure 1 summarizes the locations of all the measurements presented in this paper, i.e. over three continents, Europe, Asia, and Africa~~)~~. Except for the SHIVA winter campaign, all campaigns were conducted in late spring or summer. In general, most campaigns were conducted in Europe, except ~~for~~ the SHIVA and ~~the~~ DACCIWA campaigns conducted in Southeast Asia and West Africa, respectively. A wide area was covered by the measurements, for example, including tropical regions (SHIVA and DACCIWA) and northern mid-latitude regions (all others). Measurements during the MAGIC 2021 also covered a part of the northern high-latitude region. In general, the CO level depends on the pollution, with the highest values in the boundary layers (< 2 km altitude) of areas influenced by anthropogenic activities. The upper troposphere (> 6 km altitude) is cleaner (except for MAGIC 2021 high latitude area influenced by long range transport: see more detail in Sections 3.8 and 3.10). Also, ~~I~~it is worth noting that two inter-continental flights, one from Europe to South Asia and the other from Europe to West Africa, were conducted during the transition flights for SHIVA and DACCIWA projects (more details in Section 3.9).

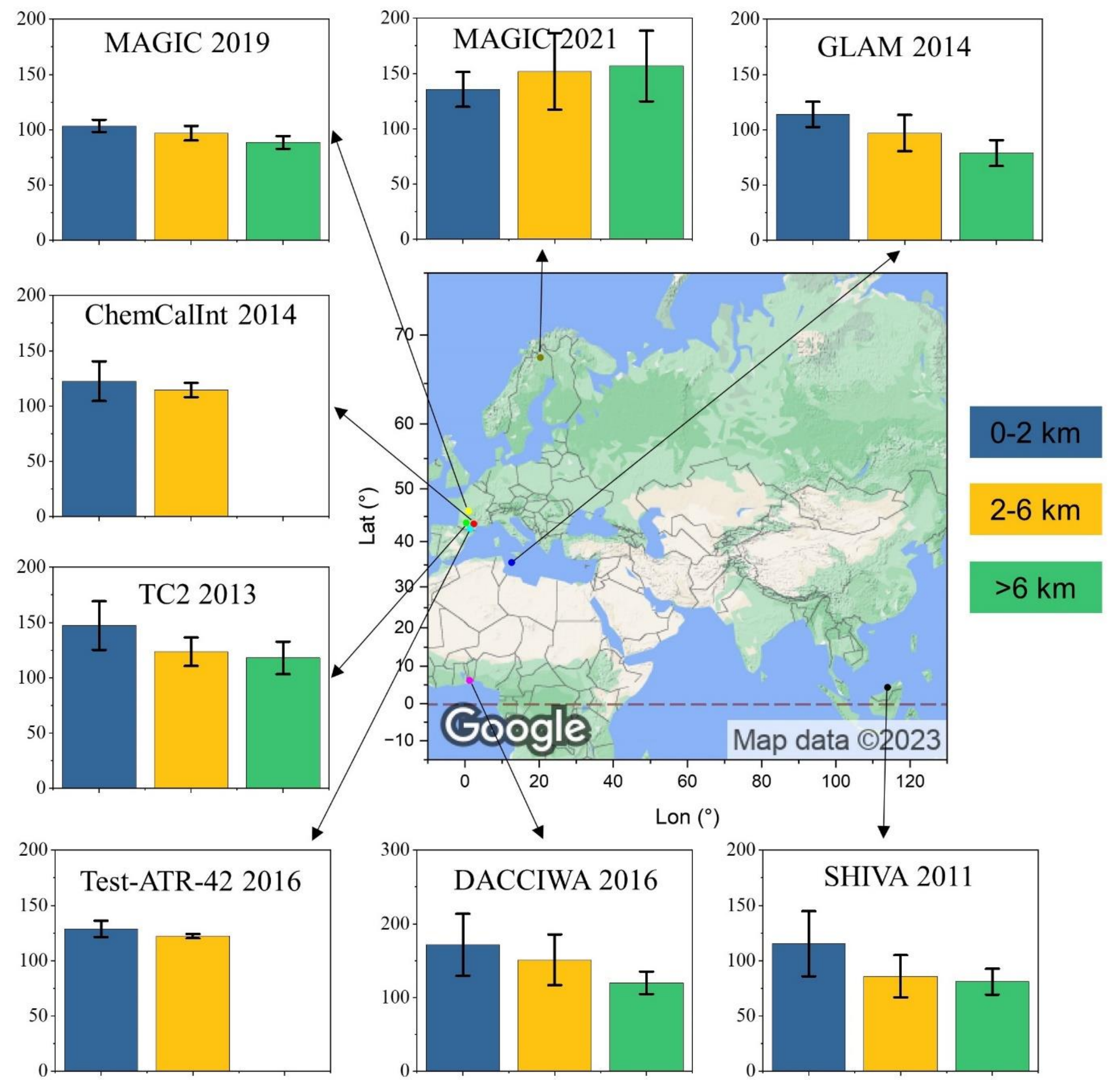

Figure 1. Locations of the main airport used for each project. Map copyright: © GoogleMap. The same airport in Toulouse was used for TC2-2013, ChemCallnt-2014, and Test ATR-2016, then the overlapped points are offset and plotted horizontally. Lampedusa E Linosa airport is selected for GLAM-2014 as it is at the center of the measurement area. Barplots show the average CO levels in the boundary layer (0-2 km), lower free troposphere (2-6 km) and upper free troposphere (>6 km) for each project.

Table 2: Information about SPIRIT CO measurements.

Projects	Period	Aircraft	Number of Flights	Region	Duration (h)
SHIVA (2011)	Nov. – Dec. 2011	A	16	1º – 8º N, 114º – 122º E	58.5
SHIVA (2011)[a]	Nov. 2011	A	5	4º – 49º N, 11º – 115º E	17.0
TC2 (2013)	Mar. – May 2013	B	11	40º – 48º N, -8º – 9º E	26.8
ChemCalInt (2014)	May 2014	C	4	42º – 46º N, 0º – 6º E	13.9
GLAM (2014)	Aug. 2014	B	9	33º – 46º N, -1º – 35º E	24.3
Test sur ATR-42 (2016)	May 2016	C	1	42º – 44º N, 0º – 2º E	2.3
DACCIWA (2016)	Jun. – Jul. 2016	A	14	3º – 11º N, -5º – 3º E	51.7
DACCIWA (2016)[b]	Jun. 2016	A	5	5º – 52º N, -18º – 13º E	13.3
MAGIC (2019)	Jun. 2019	B	3	43º – 49º N, -2º – 4º E	9.7
MAGIC (2021)	Aug. 2021	C	6	64º – 69º N, 6º – 27º E	21.4
Total			**74**		**208.8**

[a]: 5 inter-continent flights from Europe to Asia; [b]: 5 inter-continental flights from Europe to Africa.

A: Falcon-20 DLR; B: Falcon-20 SAFIRE; C: ATR-42 SAFIRE

3.1 SHIVA – Malaysia (2011)

In the framework of the SHIVA (**S**tratospheric Ozone: **H**alogen **I**mpacts in a **V**arying **A**tmosphere) project of the European Commission FP7-Enviroment Program (https://cordis.europa.eu/project/id/226224, last access: ~~18 February~~July 18, ~~-~~2023), 16 research flights were conducted using the German Aerospace Agency (DLR) Falcon-20 aircraft in Malaysia (~~Borneo island~~Borneo Island) between ~~16~~ November 16 and ~~11~~ December 11, 2011. The three-dimensional trajectories with CO volume mixing ratios (vmr) are displayed in the Supplementary Information in Figures S1 to S16. Measurements during the 5 inter-continental flights from Europe to Asia are presented in Section 3.9.

The SPIRIT instrument was on board during all the flights (58.5 hours) for measurements of CO vmr. Figure 2~~Figure 2Figure 1~~ shows all the trajectories of those flights. Most measurements were conducted along the coastal lines of Malaysia and Brunei, with several flights reaching the hinterland of this island and several flights crossing the South China Sea and reaching the region of Malacca Strait. The measurement domain represents a typical tropical region (latitude scale: 1º -7º N).

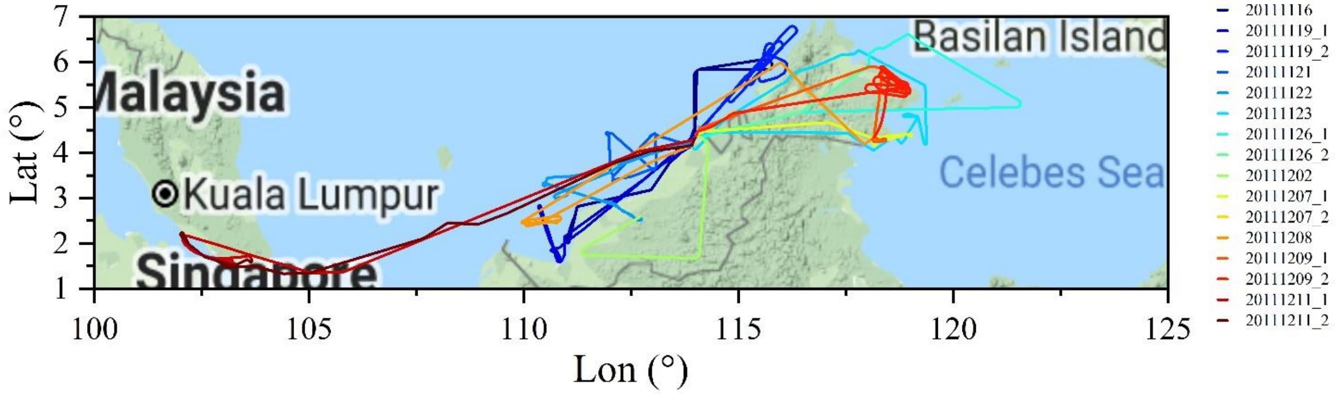

Figure 22~~1~~: Flight trajectories during the SHIVA 2011 campaign. Map copyright: © GoogleMap.

Figure 3~~Figure 3Figure 2~~ exhibits the trajectory of the first scientific flight on ~~19~~ November 19, 2011, which gives an insight of the CO level in the boundary layer and free troposphere of the Borneo island. The aircraft took off from Miri airport (Malaysia), gradually increasing its altitude to 8400 m asl. It flew along the coastal line of the Sarawak state (Malaysia) and reduced its flying height before reaching the southwest of the Sarawak state. Then, after conducting horizontal measurements over the ocean boundary layer, the aircraft increased its flying height and flew back to Miri airport. After about 2.4 hours of measurements, the aircraft landed at Miri airport. During the flight, the observed CO reached 140 ppbv in the boundary layer (0-2 km) and was lower than 100 ppbv in the lower free troposphere (2-6 km), but relatively stable, around 100 ppbv at ~8 km. Moreover, The polluted air in the boundary layer can also be lifted by convection to affect the upper troposphere. For instance, based on the measurements on flights referenced as 20111119_2~~b~~, 20111209, 20111211_1, and 20111211_2 in the SHIVA project, Krysztofiak et al. (2018) found correlated enhancements of CO, CH_4, and short-lived halogen species (i.e., CH_3I and $CHBr_3$) at heights around 11-13 km asl, which is interpreted as the fingerprint of the vertical transport from the boundary layer driven by the convective updraft. The fraction of air mass in the from the boundary layer can reach 67%, indicating the significant impact of the convective system on the composition of the upper troposphere in the tropical regions (Hamer et al., 2021).

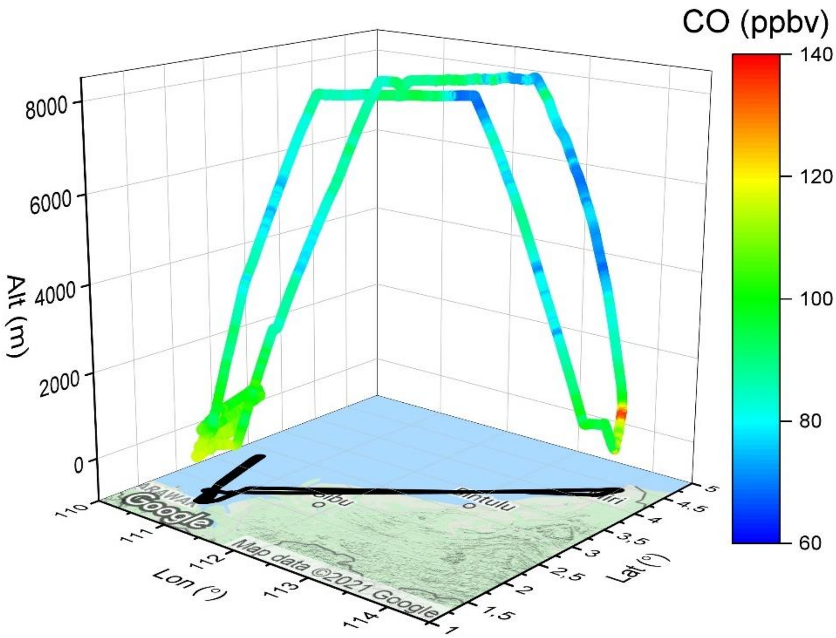

Figure 3~~32~~: Flight trajectory colored by CO levels on flight-SHIVA_20111119_1. Map copyright: © GoogleMap.

3.2 Traînées de Condensation et Climat: TC2 - France (2013)

In the framework of the contrails and climate project TC2 (Traînées de Condensation et Climat, http://www.cerfacs.fr/TC2/index.html, last access: ~~18 February~~July 18, ~~-~~2023), 11 flight measurements (Figures S17-S27 in the Supplementary Information) were conducted from ~~12~~ March 12 to ~~31~~ May 31, 2013, with a total measurement duration of around 27 hours. For each flight, the Falcon-20 aircraft with SPIRIT on board flew in the wake of commercial flights, most of which are on the Paris – North Africa route. This allows the detection of aircraft emissions and the study of the air mass aging of contrails. As shown in Figure 4~~Figure 4Figure 3~~, most measurements were conducted in the region over Toulouse and the South~~-West~~ west of France, ~~but~~ and several flights reached the Atlantic Ocean and the Mediterranean Sea.

Figure 5~~Figure 5Figure 4~~ shows the measurements during the 20 March 2013 flight, since they are at the heart of the study, i.e., the emissions of NO_2 and CO by aircraft. Sudden increases of NO_2 by a few ppb (from a background level of less than 0.5 ppb) were observed when chasing aircraft a few minutes in the wake behind them, but no increase of CO as seen here in the middle of ceiling altitude (10.5 km), suggesting complete combustion in the aircraft engines or very rapid dilution process if there are emissions.

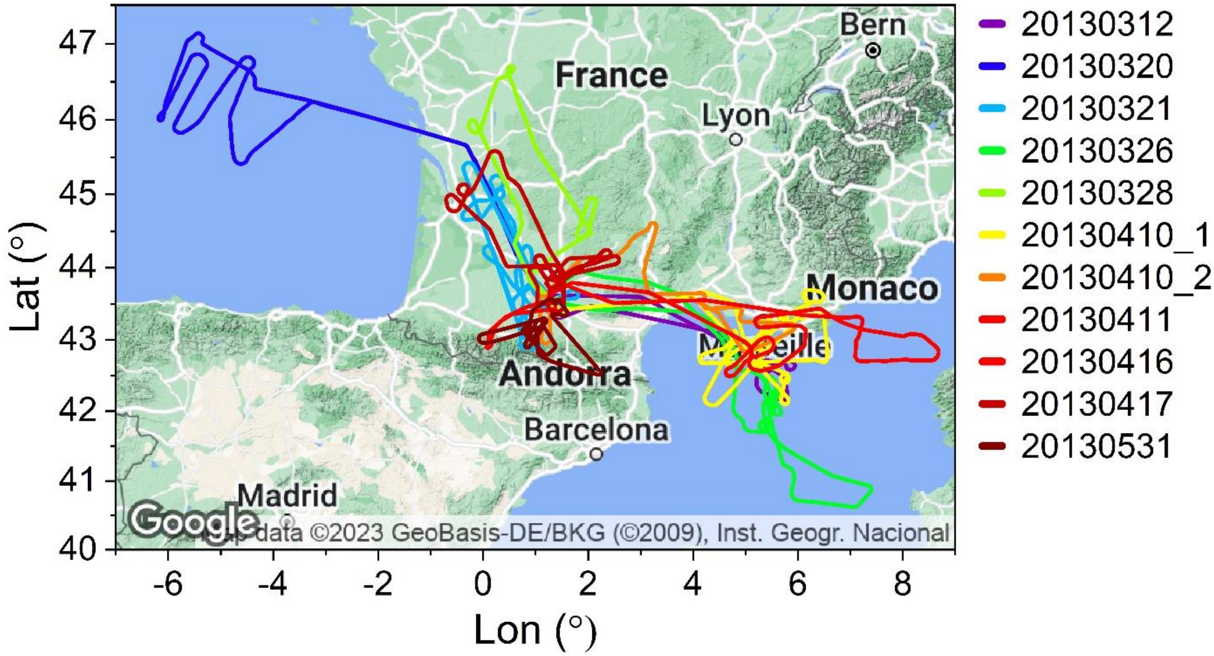

Figure 44~~3~~: Flight trajectories during the TC2 2013 campaign. Map copyright: © GoogleMap.

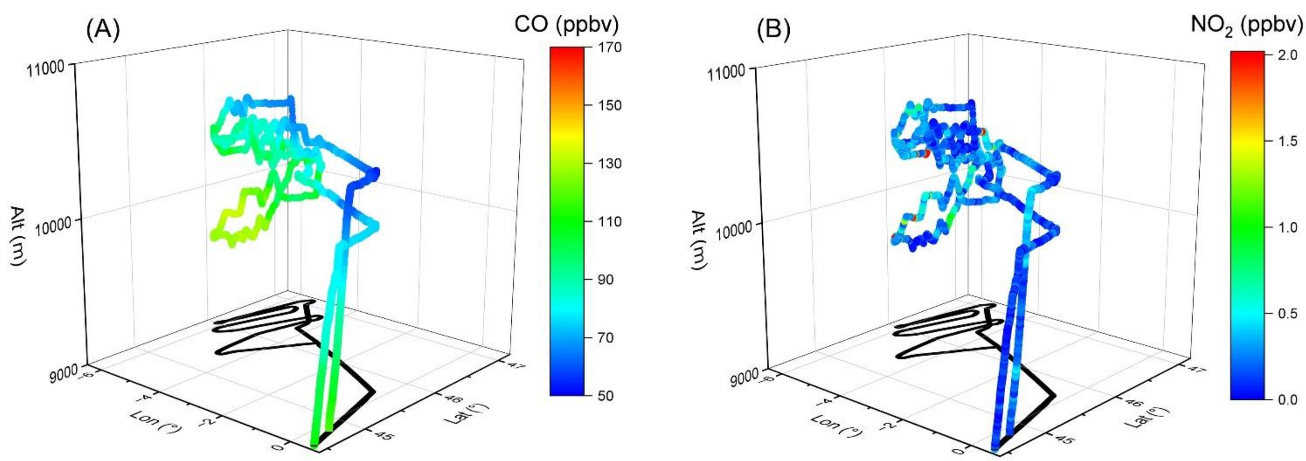

Figure 55~~4~~: Flight trajectory colored by CO and NO_2 vmr on flight-TC2_20130320_1. Three NO_2 vmr sudden increases up to more than 2 ppbv (symbolised by red dots) are seen when our research aircraft was inside the contrails emitted by commercial aircraft, whereas there was no such increase in CO level. Map copyright: © GoogleMap.

3.3 ChemCalInt - France (2014)

The ChemCalInt project is~~,~~ a French initiative part of the European JRA TGOE in EUFAR for the traceability in gas-phase observations' on-board research aircraft~~, –~~. This project was built to compare the measurements of CO and CH_4 by different airborne instruments in order to ensure their consistency and their performance and to implement adapted calibration procedures in future campaigns. Figure 6~~Figure 6Figure 5~~ shows all the flight trajectories during this project. Four flights were conducted in southern France, generally between/around Toulouse, Clermont-Ferrand, and the Pyrenees Mountains (Figures S28-S31). ~~This project was built to compare the measurements of CO and CH_4 by different instruments in order to ensure their consistency and their performance and to implement adapted calibration procedures in future campaigns.~~

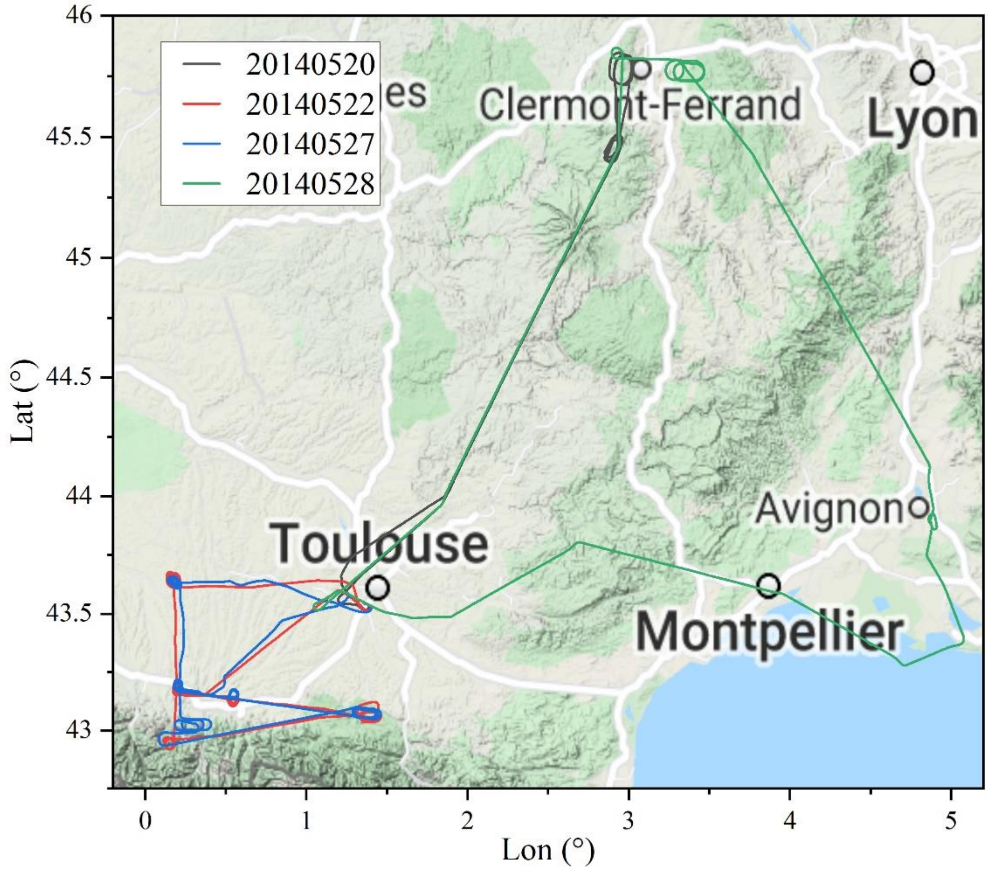

Figure 6~~65~~: Flight trajectories during the ChemCalInt 2014 campaign. Map copyright: © GoogleMap.

In Figure 7~~Figure 7~~, CO measurements along with the flight trajectories on ~~22~~ May 22, 2014 are shown ~~a~~since ~~i~~they represent~~s~~ the typical CO distribution and level in this region. The aircraft flew to the meteorological station of Peyrusse-Vieille, the Centre de Recherches Atmosphériques de Lannemezan (OMP), the Pyrenees National Park, and the Regional Natural Park of the Ariegean Pyrenees. Over this natural park, a background measurement of the vertical profile of CO (i.e., < 115 ppbv) was ~~conduct~~observed. In general, the measured CO vmr during this flight was lower than 120 ppbv, with an exception over Toulouse. This is the typical CO level in Southwest France with no big cities and no significant anthropogenic emissions in this region. The vertical homogeneity of CO over the Regional Park is representative of CO distribution over this region as seen in Section 3.9 and Figure 25~~Figure 25~~.

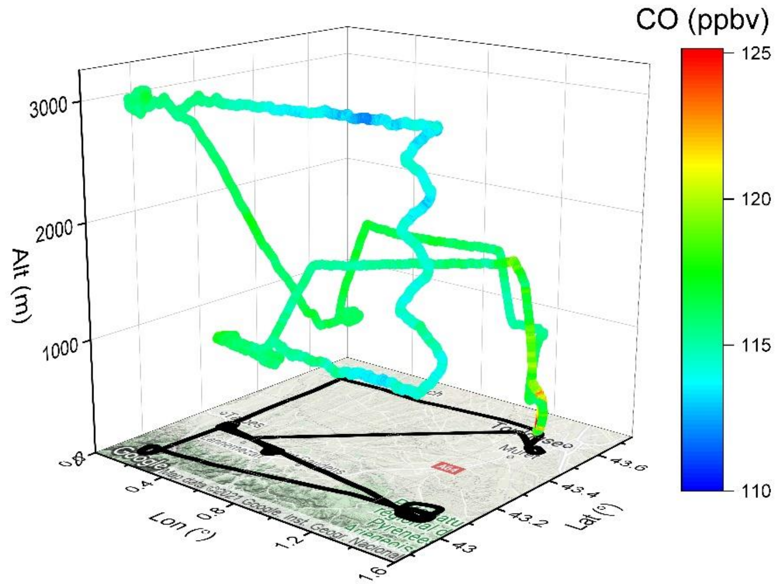

Figure 7~~76~~: Flight trajectory colored by CO levels on flight-~~ ~~ChemCalInt_20140522_1. Map copyright: © GoogleMap.

3.4 ChArMEx – GLAM Mediterranean (2014)

Within the frame of the MISTRALS-ChArMEx program (https://programmes.insu.cnrs.fr/mistrals/programmes/charmex/, last access: ~~18 February~~July 18, 2023), the GLAM experiment (**G**radient in **L**ongitude of **A**tmospheric constituents above the **M**editerranean basin, https://www.safire.fr/content_page/32-campagnes-passees/106-glam.html?lang=fr, last access: ~~18 February~~July 18, 2023) aims to describe the high-resolution horizontal and vertical distribution of pollutants over the Mediterranean Basin along an East-West axis (Ricaud et al., 2018; Brocchi et al., 2018). As shown in Figure 8~~Figure 8Figure 7~~, the measurement domain of the 9 flights covers the target region, west from the France-Spain border and east to Cyprus (Figures S32-S40). Measurements were mostly conducted over the sea, with some exceptions for islands including Balearic Island, Sardinia Island, Crete Island, and Cyprus Island, drawing the whole picture of CO profiles over the Mediterranean Basin.

Data obtained in this project can be used to study anthropogenic emissions in the Mediterranean region, for which measurements on ~~8~~ August 8, 2014 ~~As~~ provide an excellent example~~,~~. Figure 9~~Figure 9Figure 8~~ shows measurements during this flight with a measurement area over Cyprus and surrounding regions. High levels of CO up to 130 ppbv were observed in the boundary layer (< ~~2000~~ 2 km altitude) over the coastal regions of south-eastern Cyprus and the ~~ocean~~ sea on the west of Cyprus, indicating impacts of ~~anthropogenic~~ urban and shipping emissions, respectively.

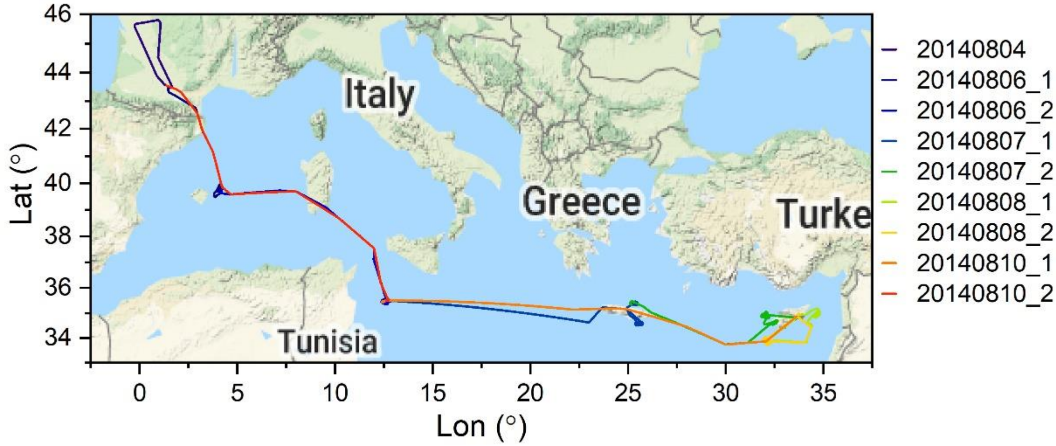

Figure 88~~7~~: Flight trajectories during the GLAM-2014 campaign. Map copyright: © GoogleMap.

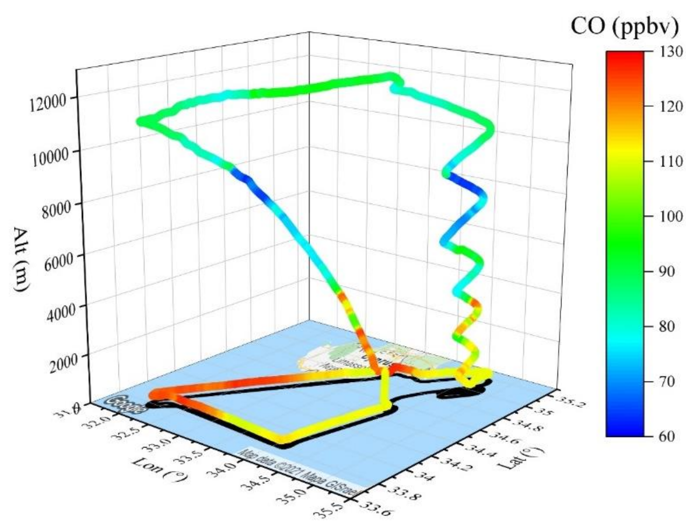

Figure 99~~8~~: Flight trajectory colored by CO levels on flight-GLAM_20140808_1. Map copyright: © GoogleMap.

3.5 Test-ATR-42 (2016)

The Test-ATR-42 project aims to test the performances of SPIRIT, with more intensive calibrations during the flight compared to other field campaigns, as detailed in Catoire et al. (2017). As shown in Figure 10~~Figure 10Figure 9~~, 17 calibrations with the WMO CO standard of 136.1 ± 0.4 ppbv were made during the flight on ~~5~~ February 5, 2016. Those calibrations cover both ascending and descending of the aircraft in the altitude range of 0 – 6 km, showing no dependence of the results on temperature or pressure. Each time the sampling inlet is connected to the cylinder containing the WMO CO standard, measurements rapidly (in 10 s) reach a stable value around 140 ppbv, with a small scattering (< 1 ppbv at 1σ, Figure 11~~Figure 11Figure 10~~), highlighting the accuracy and reproducibility of SPIRIT in aircraft measurements.

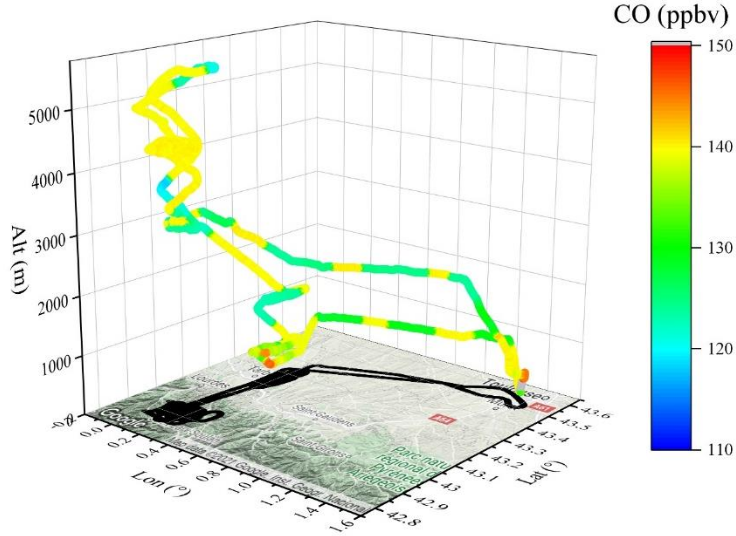

Figure 10~~109~~: Flight trajectory colored by CO levels on flight-Test-ATR-42_20160205_1. Map copyright: © GoogleMap.

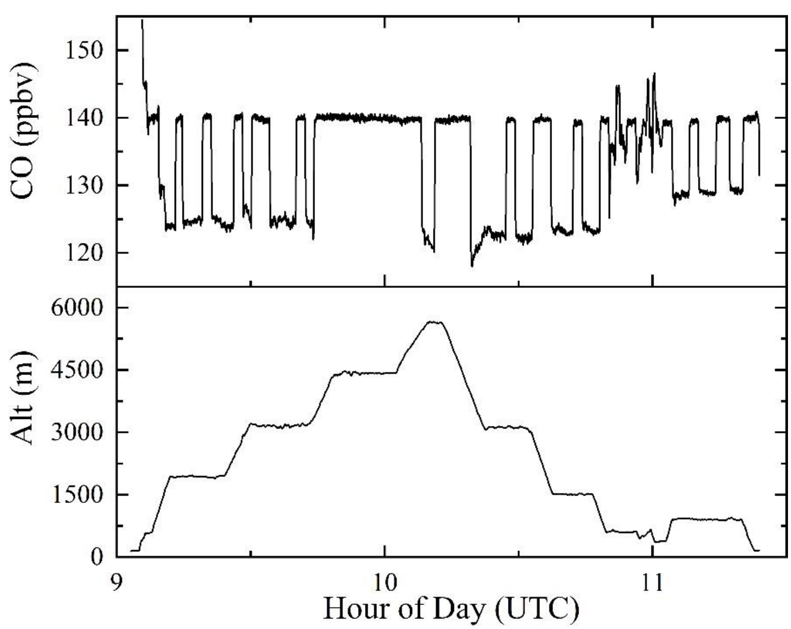

Figure 11~~11~~~~10~~: Time series of CO and altitude on flight- Test-ATR-42_20160502_1.

3.6 DACCIWA – West Africa (2016)

In the summer of 2016, the EU FP7 ~~EU~~ project DACCIWA (Dynamics-Aerosol-Chemistry-Cloud Interactions in West Africa) was implemented to investigate the atmospheric impacts of anthropogenic and natural emissions in West Africa, where high-quality airborne measurements are quite scarce (Knippertz et al., 2015; Hahn et al., 2022; Taylor et al., 2019; Wu et al., 2021; Formenti et al., 2019; Redemann et al., 2021; Haywood et al., 2021). 14 flights (> 50 h measurements; Figures S42-S55) were conducted in coastal regions as well as the surrounding Atlantic Ocean and continental regions of West Africa (Figure 12~~Figure 12~~~~Figure 11~~). In general, CO levels in West Africa are higher than those in the Mediterranean Basin (Section 3.4).

For example, Figure 13~~Figure 13~~~~Figure 12~~ shows a flight along the coastal lines and over the Gulf of Guinea. This represents a typical measurement as it is impacted by different types of pollutions ~~anthropogenic emissions, ship emissions, and biomass burning emissions~~. High CO values (200 – 300 ppbv) were observed within 2 km above Lomé (~~capital of~~ Togo), suggesting ~~anthropogenic~~ urban emissions and/or shipping emissions (see ship positions near the Lomé port in Figure S65). Moreover, Brocchi et al. (2019) found that offshore oil rig emissions (e.g., CO, NO_x, and aerosol within the boundary layer) also showed an impact on regional air quality. The pollutants emitted above the ocean by ships and oil rigs are thus transported along the West African Monsoon (south-westerly in summer) to the continents (Kniffka et al., 2019; Brocchi et al., 2019), affecting the air quality in those regions. Notably, a pollution plume caused by biomass burning emissions, with aerosols visible live through the aircraft window and higher CO levels (150 – 200 ppbv) than the background (100 – 150 ppbv, Figure 13~~Figure 13~~~~Figure 12~~), was observed at 2.8 – 4.0 km and was captured again at a similar altitude but further from the coast~~, which is caused by biomass burning emissions~~.

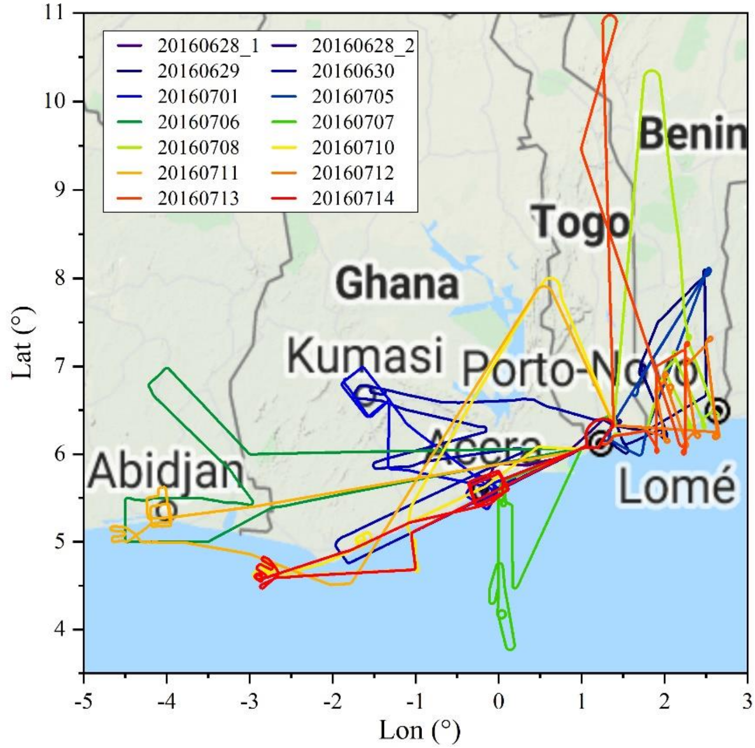

Figure 12~~12~~~~11~~: Flight trajectories during the DACCIWA 2016 campaign. Map copyright: © GoogleMap.

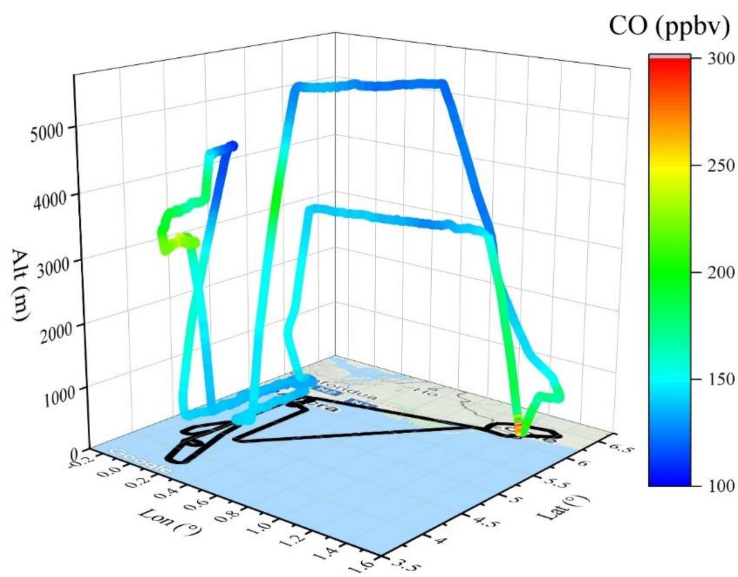

Figure 13~~13~~~~12~~: Flight trajectory colored by CO levels on flight-DACCIWA_20160707_1. Map copyright: © GoogleMap.

Local emissions were frequently observed during this campaign. For instance, as shown in Figure 14~~Figure 14Figure 13~~, the flight on ~~12 ~~July 12, 2016 allowed intensive measurements between Lomé (Togo) and Porto-Novo (Benin). Most measurements over the continent showed higher CO levels than those over the ocean, with several CO peaks up to 200 ppbv occasionally accompanied by peaks of NO_2 and SO_2 (not shown). Those peaks were observed within the boundary layer, indicating the impact of anthropogenic emissions in this region. These measurements are important for documenting and understanding local air pollution, considering that the increasing population and economy lead to more anthropogenic emissions (Knippertz et al., 2015). Also, aerosol pollution traced by CO levels (> 155 ppbv) is shown to slightly enhance atmospheric cooling by low-level clouds in tropical West Africa by increasing the droplet number concentration and reducing the droplet size in the clouds (Hahn et al., 2023; Taylor et al., 2019).

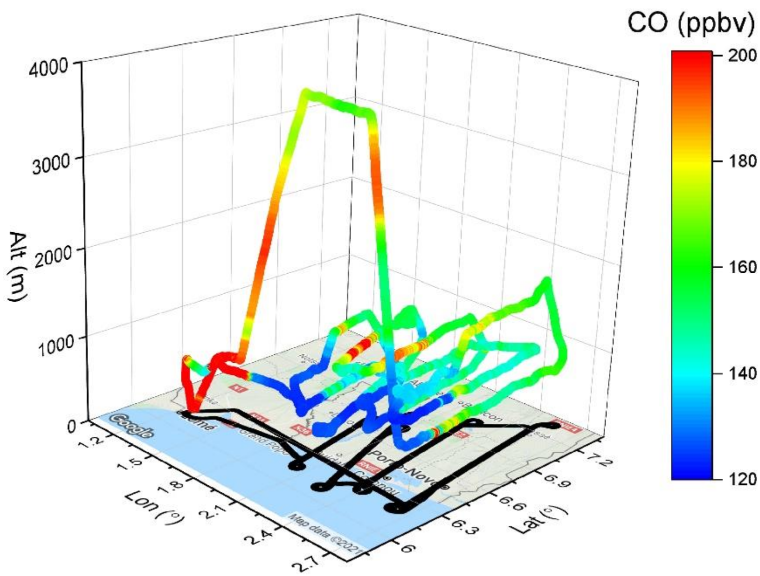

Figure 14~~1413~~: Flight trajectory colored by CO levels on flight-DACCIWA_20160712_1. Map copyright: © GoogleMap.

3.7 MAGIC (2019)

MAGIC (Monitoring Atmospheric composition and Greenhouse gases through multi-Instrument Campaigns, https://magic.aeris-data.fr/, last access: ~~18 February~~July 18, 2023) is a long-term CNES-CNRS French project, with two main goals: (i) to better understand the vertical exchange of greenhouse gases along the atmospheric column, in connection with atmospheric transport, sources and sinks of the gases at the surface and in the atmosphere; (ii) to contribute to the validation of satellite products of IASI-MetOpC (CNES), Tropomi-Sentinel 5P (ESA), GOSAT 2 (JAXA), and OCO-2 (NASA), and to prepare the validation of space missions MicroCarb, IASI-NG (CNES), and Merlin (CNES-DLR) dedicated to the monitoring of greenhouse gases and other species. In June 2019, the MAGIC campaign was conducted in France, with three flights over the Toulouse-La Rochelle-Orléans-Clermont-Ferrand region (Figure 15~~Figure 15Figure 14~~ and Figures S56-S58 for 3D trajectories with CO vmr).

Similar to the Test-ATR project (Section 3.5), intensive in-flight calibrations were conducted, which led to the plots of CO versus flight trajectories (Figures S56 – S58). Figure 16~~Figure 16Figure 15~~ shows the measurements during calibration for the two flights on ~~18~~ June 18, 2019. The eight calibration processes cover ascending, descending, and cruise periods in the altitude range of 0 – 12 km. This results in an agreement between the WMO CO_X2014A standard and the SPIRIT instrument within 3.2 ± 0.6 ppbv (1σ) out of 149.0 ppbv, confirming the accuracy and stability of SPIRIT for aircraft measurements.

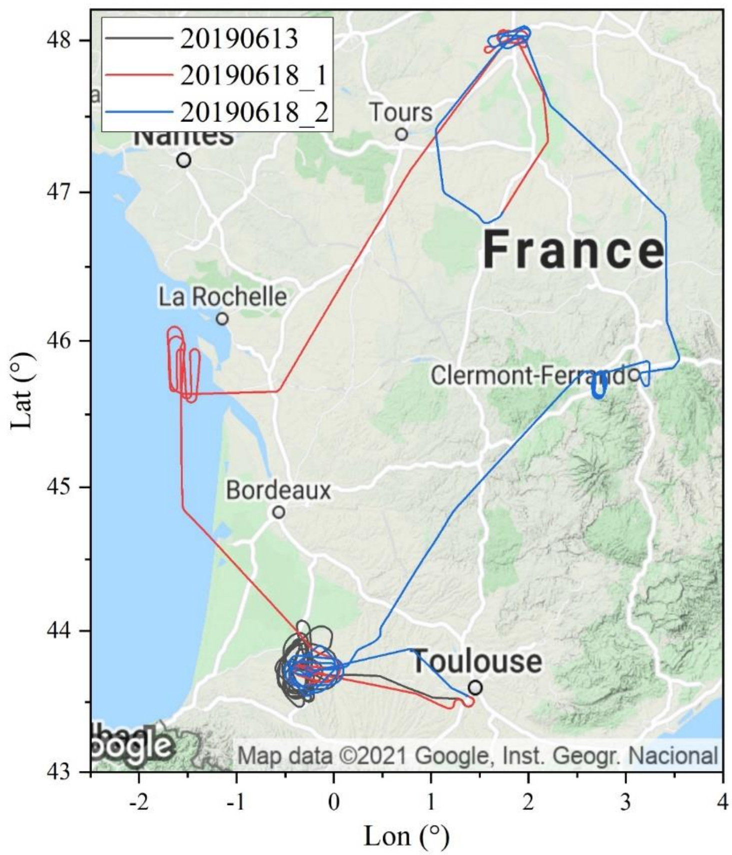

Figure 15~~1514~~: Flight trajectories during the MAGIC 2019 campaign. Map copyright: © GoogleMap.

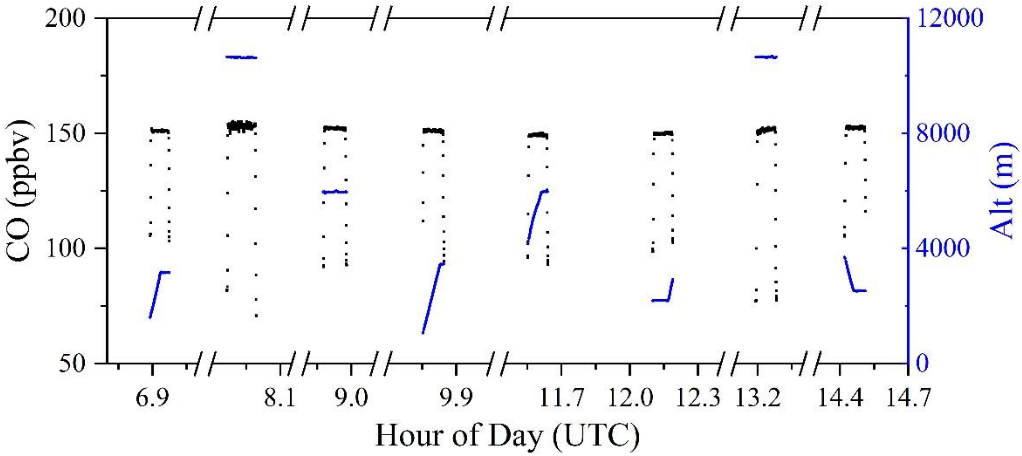

Figure 16~~16~~~~15~~: Time series of CO values (black dot) and altitude (blue dot) during calibration on flight~~-~~MAGIC_~~-~~20190618_1 and MAGIC_20190618_2.

3.8 MAGIC (2021)

In the continuation of the MAGIC 2019 project above, exploring high latitude regions is of interest since the~~y~~se ones are warming faster than the ~~global~~ average, as a result of anthropogenic, natural emissions and transport of pollution. However, airborne measurements are scarce in high-latitude regions, which limits the understanding of the horizontal and vertical distribution of pollution and causes problems in validating satellite performance in those regions. In August 2021, the international MAGIC-2021 campaign (https://magic.aeris-data.fr/, last access: ~~18~~ July~~anuary~~ 18, 2023) took place in Kiruna (67.9°N, 21.1°E), Sweden. As shown in Figure 17~~Figure 17~~~~Figure 16~~, the six flights mainly ~~took~~ performed measurements over northern Sweden and northern Finland, with one flight reaching the Norwegian Sea (Figures S59-S64).

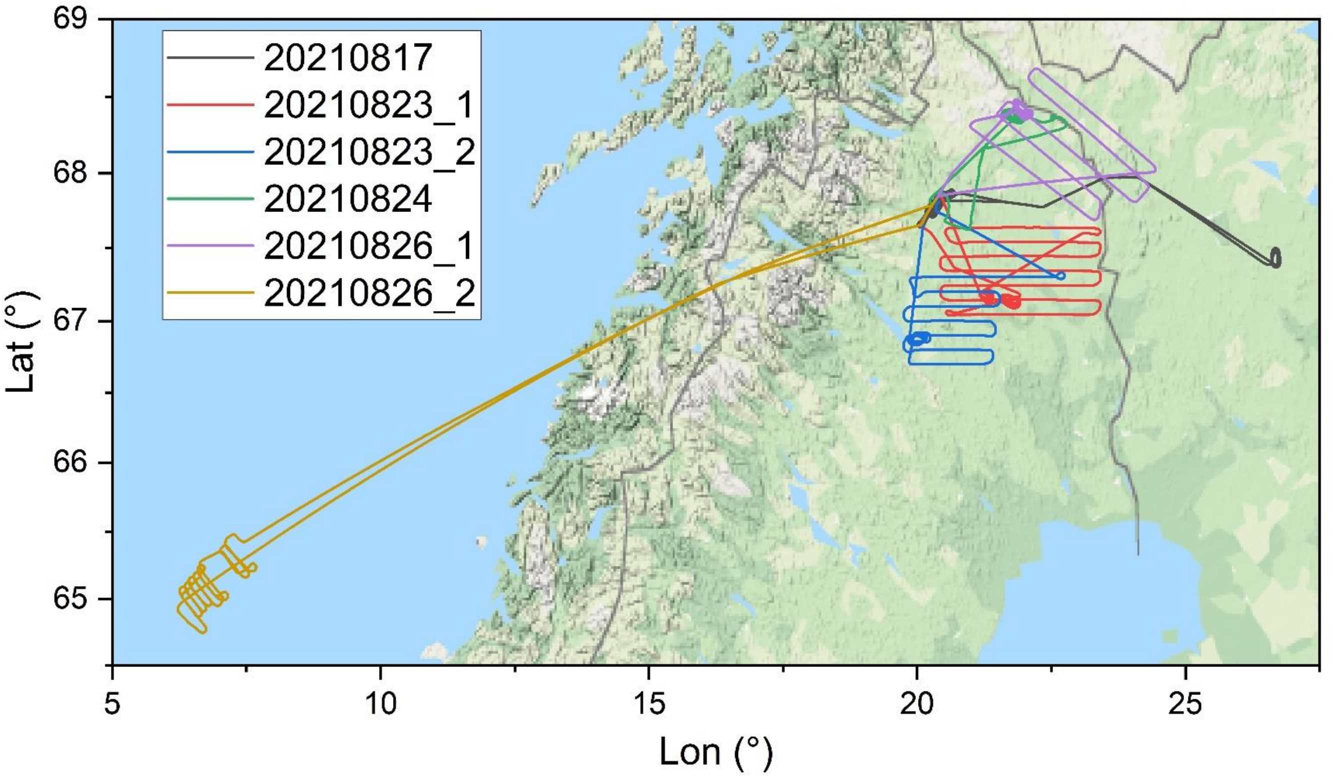

Figure 17~~17~~~~16~~: Flight trajectories during the MAGIC 2021 campaign. Map copyright: © Google Map.

On the morning of ~~23~~ August 23, 2021, a~~n aircraft~~ flight was designed to provide ~~horizontal and vertical~~ measurements ~~that benefit~~for the validation of satellite products aforementioned in Section 3.7. Intensive vertical and horizontal measurements were carried out, synchronized with several satellite overpasses~~-~~. As shown in Figure 18~~Figure 18Figure 17~~, the aircraft ~~spiraled~~spiralled up, achieving two vertical profiles of measurements within an altitude range of 0 – 7.5 km asl. At the maximum altitude, the aircraft descended to 4.5 km asl and conducted intensive horizontal measurements in the region of 67.0 – 67.6 ºN and 20.0 – 23.5ºE. CO vmr was mostly around 150 – 250 ppbv in this region. After that, it ~~spiraled~~spiralled up again to 7.5 km asl, followed by spiraling down to the ground level before landing back at Kiruna airport. CO was mostly around 150 ppbv within the boundary layer of ~2 km asl. However, it increased with altitude above the boundary layer (peak of 285 ppbv at ~5.5 km asl, Figure 29~~Figure 29Figure 29~~), likely due to long-range transported fire pollution (study in progress).

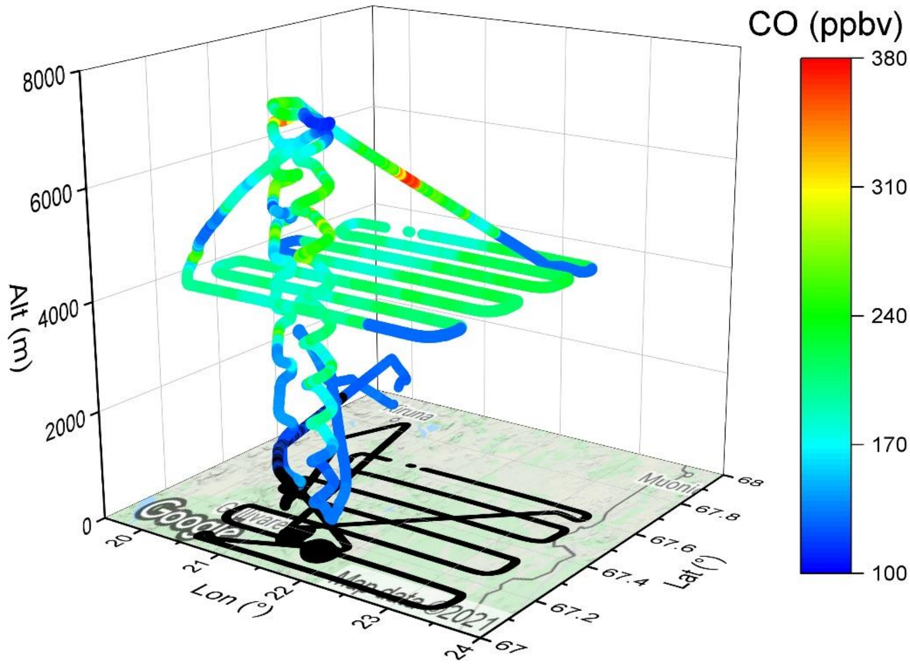

Figure 18~~18~~~~17~~: Flight trajectory colored by CO levels on flight-MAGIC_20210823_1. Map copyright: © Google Map.

In addition to long-range transport, ~~Local~~ local emissions from fires were also observed. Measurements on August 26 showed the impact of two pollution sources. ~~On 26 August at~~ At 9:30 (half an hour after starting the 3.6-hour flight-20210826_1) on ~~26~~ August 26, a fire caused by a rocket engine test occurred at the Swedish Space Corporation Esrange base (67.9 ºN, 21.1 ºE), which burned parts of the launching facility for sounding rockets and parts of the nearby buildings (red star in Figure 19~~Figure 19Figure 18~~). The plume of this fire was captured by our measurements. As shown in Figure 19~~Figure 19Figure 18~~, the aircraft took off at Kiruna ~~airport~~ Airport at around 9:05 a.m. (local time). Around 5 min after the take-off, high CO peaks of more than 200 ppbv were observed at an altitude of 2000 – 2750 m asl, which is nearly above the location of the fire at the Esrange base. The plume was also frequently observed at higher altitudes, i.e., four CO peaks of above 200 ppbv were observed at around 5600 m asl and distributed on a straight line, indicating the widespread of the plume.

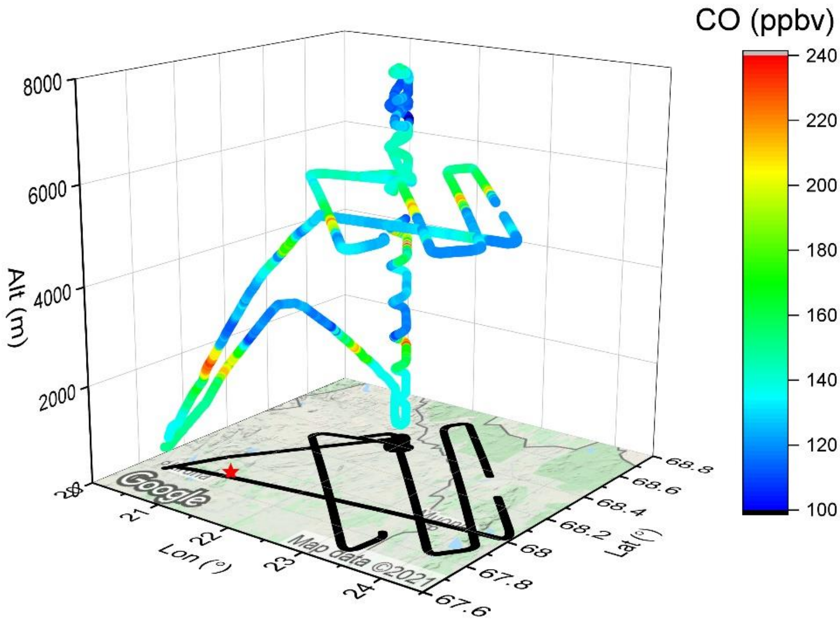

Figure 19~~1918~~: Flight trajectory colored by CO levels on flight-MAGIC_20210826_1. The red star represents the location of the fire at Esrange. Map copyright: © Google Map

3.9 Intercontinental Measurements

Two inter~~-~~continental measurements were achieved during SHIVA and DACCIWA projects. Aircraft ~~traveled~~travelled from Germany to Malaysia in South East Asia in November 2011 and to Ghana in West Africa in June 2016. Except for the landing and take-off, the measurement height was typically constant at a typical cruise altitude of ~10 km asl. This could be used for assessing the performance of chemical transport models and validating satellite observations on a global scale.

Figure 20~~2019~~: Trajectories of the two inter-continent flights during the SHIVA 2011 and DACCIWA 2016 campaigns. Map copyright: © Google Map.

3.9.1 Europe – Asia

In the framework of SHIVA, an intercontinental measurement was conducted from Munich (Germany) to Miri (Malaysia), with four stops at Larnaca (Cyprus), Dubai~~,~~ (United Arab Emirates), Hyderabad (India), and Pattaya U-Tapao (Thailand), respectively (Figure 21~~Figure 21Figure 20~~). Except for CO peaks observed after the take-off, the measured CO was typically lower than 110 ppbv. Higher CO levels (> 130 ppbv) were observed in the boundary layer over Hyderabad and U-Tapao, indicating the impacts of local anthropogenic emissions. The pollution of the boundary layer above these last two cities is clearly visible, with CO levels well above 200 ppbv. Also, before landing at Miri, a polluted plume, with significant CO enhancements from around 80 to 200 ppbv, was observed at 10680 m asl. The width of the measured plume was about 630 km, indicating a large emission event and a wide spread. The observed plume may originate from events with intensive emissions, such as wildfires and convective transport (Krysztofiak et al., 2018; Hamer et al., 2021).

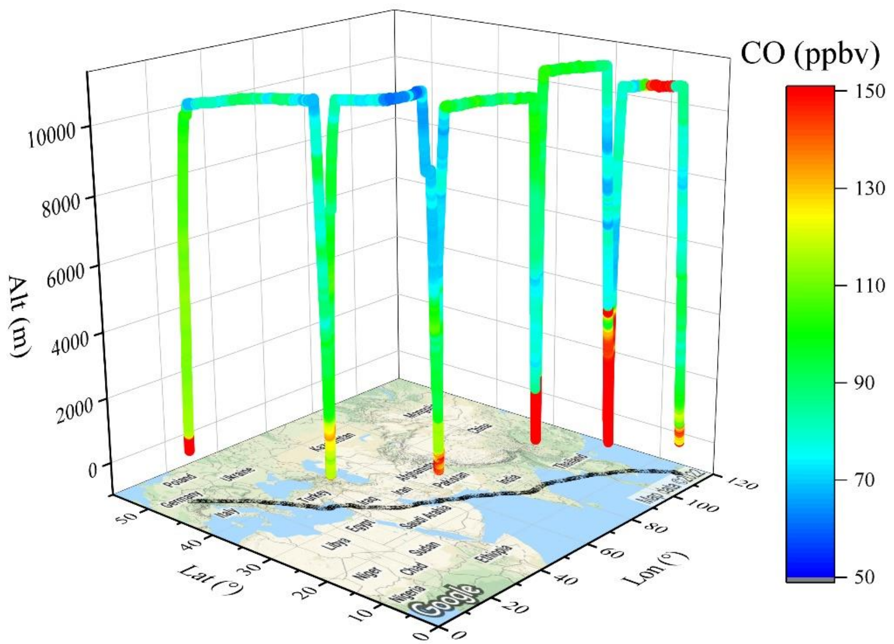

Figure 21~~2120~~: Flight trajectory colored by CO levels during the inter-continent flight during the SHIVA 2011 campaign. Map copyright: © Google Map.

3.9.2 Europe – Africa

During the DACCIWA project, the SPIRIT instrument was on board the DLR Falcon-20 for measurements during the transit flights from Germany to Togo. There were three stops: Faro (Portugal), Fuerteventura (Canary Island, Spain), and Dakar (Senegal), which allows measurements across West Europe and along the coastal lines of North and West Africa. CO measured over West Europe and North Africa is typically lower than 100 ppbv. However, higher CO levels were observed over West

Africa in the boundary layer and the upper troposphere. For example, before landing at Lomé (Togo), polluted plumes with CO up to 150 ppbv were observed in the altitude range of 20 – 4700 m asl, suggesting strong impacts of regional anthropogenic emissions.

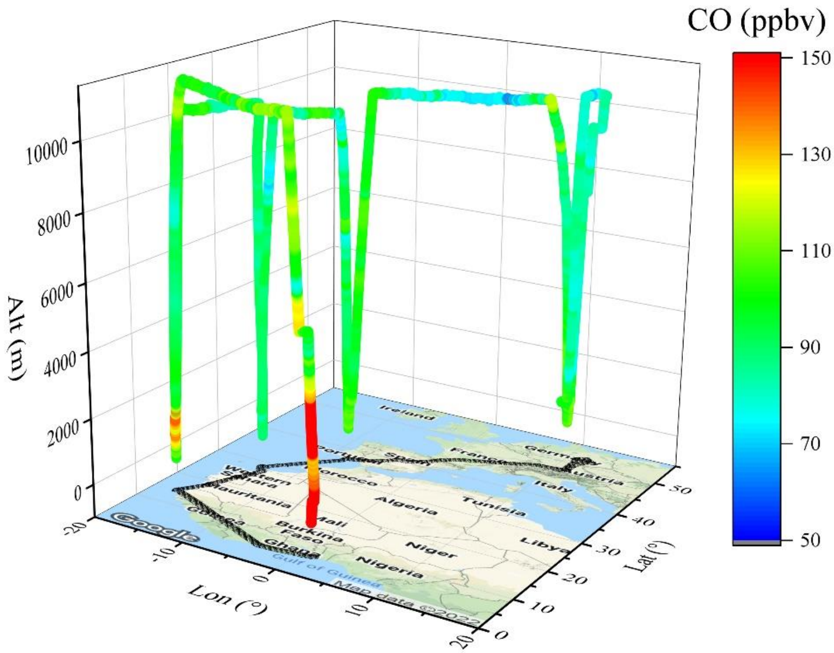

Figure 22~~2221~~: Flight trajectory colored by CO levels during the intercontinental flight during the DACCIWA 2016 campaign. Map copyright: © Google Map.

3.10 Vertical Profiles of CO in the Different Regions

~~Figure 22 summarizes the locations of all the measurements presented in this paper, i.e. over three continents (Europe, Asia, and Africa), with two inter-continental measurements (Europe-Asia and Europe-Africa).~~Figure 23~~Figure 23~~ ~~-~~ – 29 show the vertical profiles of CO observed during the campaigns. In most cases, CO levels decrease with altitude within the boundary layer (~1-2 km asl) from 100 – 200 ppbv (depending on the region) to lower values in the free troposphere, characterized as such, indicating a strong impact of anthropogenic emissions. Similar observations are made in Alaska where a nearly constant CO value was observed in an altitude range of 0 – 2 km asl (Spackman et al., 2010). However, surface CO vmr in West Africa (Figure 27~~Figure 27~~) ~~is~~are generally in the range of 200 – 300 ppbv. They are higher than in other regions. Indeed, in Europe and the whole Mediterranean ~~region~~ Basin (including TC2-2013, ChemCallnt-2014, and GLAM-2014), most surface CO levels are lower than 150 ppbv. In southern Asia, surface CO is typically at a similar level to Europe, with exceptions reaching more than 200 ppbv.

Unlike other regions, the CO vertical profile measured in high-latitude regions (Kiruna, Sweden) during the MAGIC-2021 campaign increases with altitude, with CO levels of up to 300 ppbv in the altitude range of 5000 – 7000 m asl (Figure 28). CO levels during summer seem similar or higher than inland Europe although a lower anthropogenic emission is expected, suggesting a large contribution from the transport of plumes from wildfires at high latitude regions. Indeed, assimilated TROPOMI satellite observations and CAMS model simulations ~~and~~ reported large CO emissions from wildfires over North America and Russia in July and August 2021, which led to high CO column concentrations in the Arctic region.

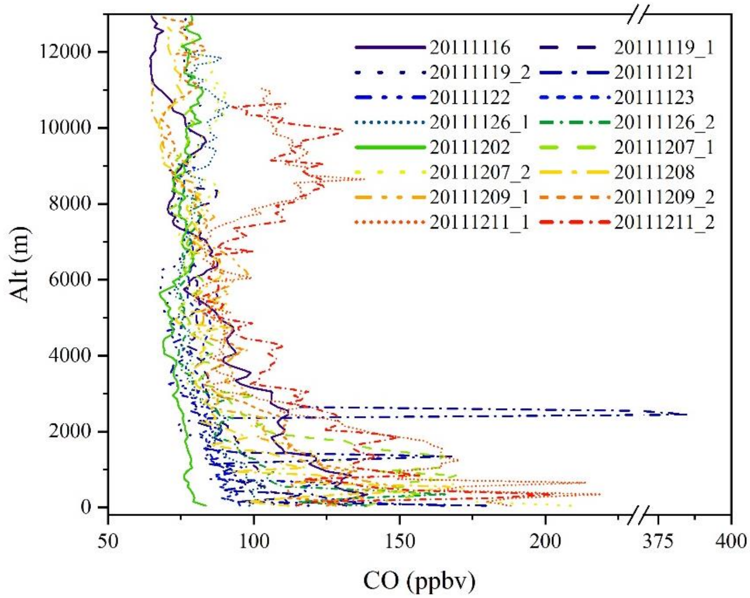

Figure 23: Vertical profiles of CO of all flights during the SHIVA (2011) campaign in Southern Asia. Vertical average bin: 100 m.

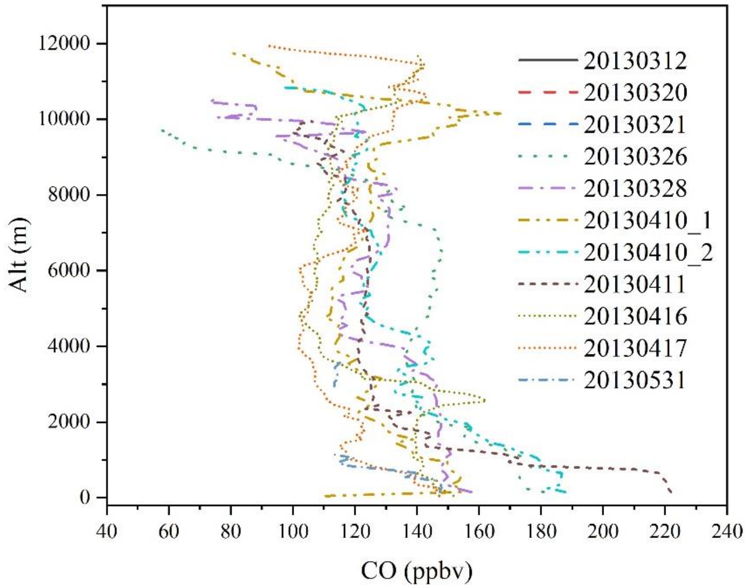

Figure 24: Vertical profiles of CO of all flights during the TC2 (2013) campaign in Southwestern France. Vertical average bin: 100 m.

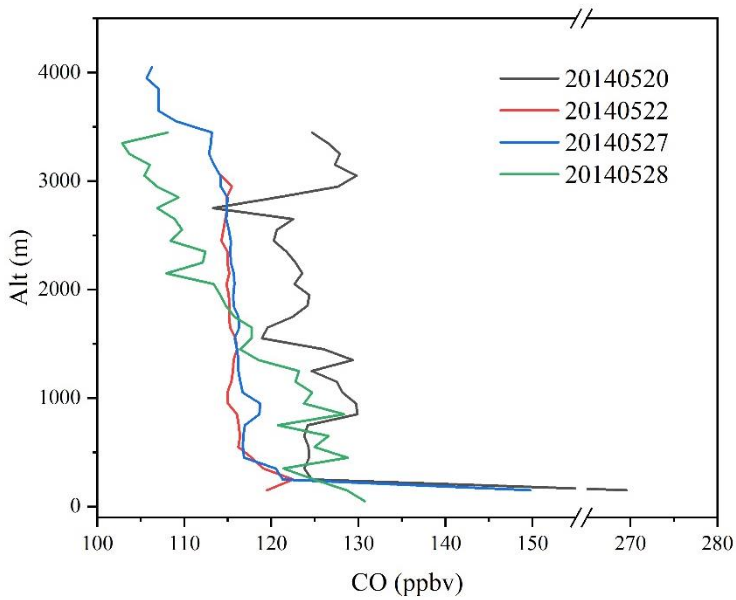

Figure 25: Vertical profiles of CO of all flights during the ChemCallnt (2014) campaign in Southern France. Vertical average bin: 100 m.

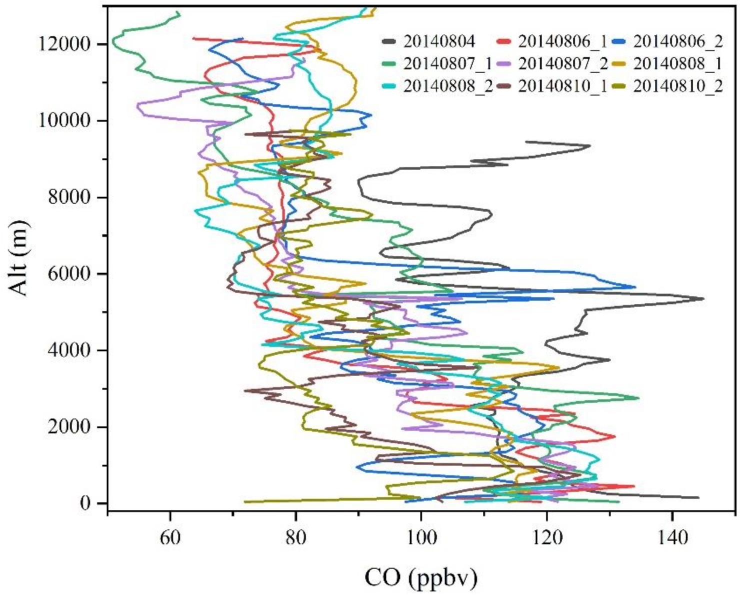

Figure 26: Vertical profiles of CO of all flights during the GLAM (2014) campaign over the Mediteraneanean Basin. Vertical average bin: 100 m.

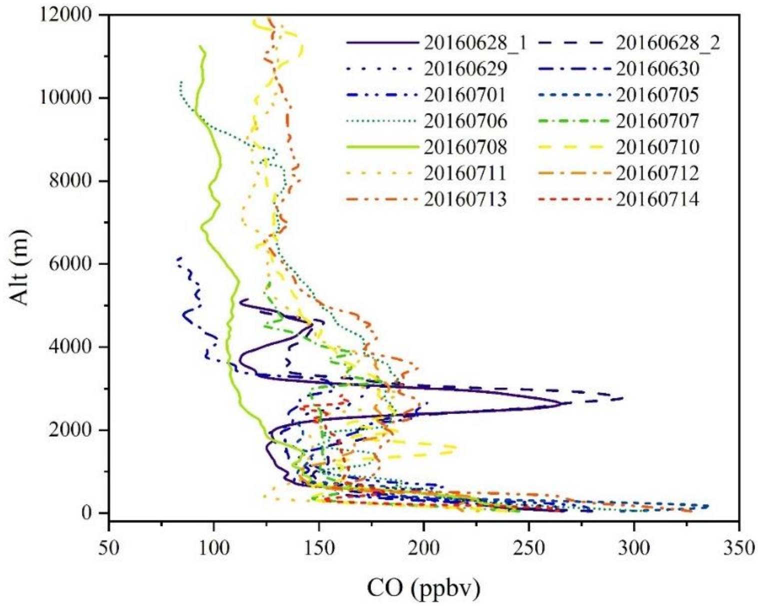

Figure 27: Vertical profiles of CO of all flights during the DACCIWA (2016) campaign in West Africa. Vertical average bin: 100 m.

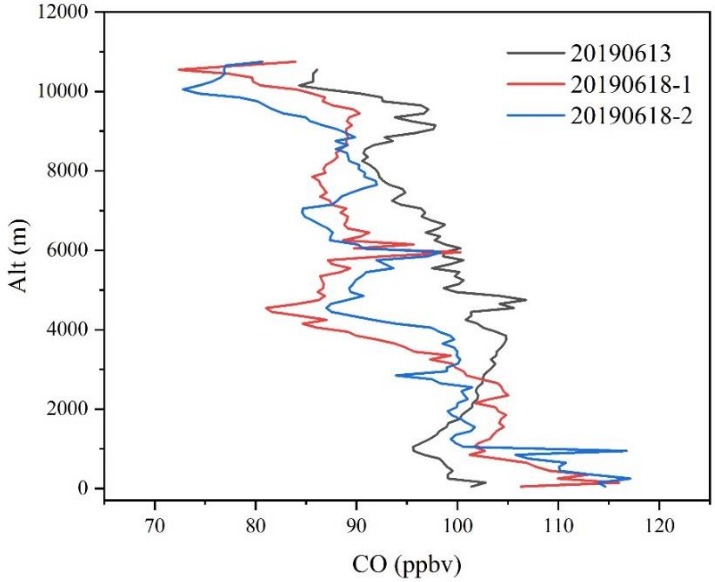

Figure 28: Vertical profiles of CO of all flights during the MAGIC (2019) campaign in France. Vertical average bin: 100 m.

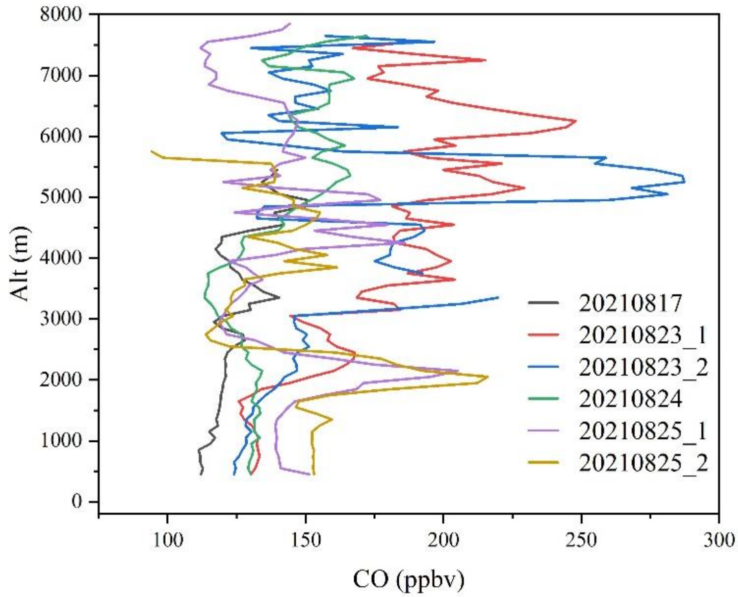

Figure 29: Vertical profiles of CO of all flights during the MAGIC (2021) campaign in Northern Sweden. Vertical average bin: 100 m.

4 Data Availability

All the data used in this study are publicly available on the AERIS database (Catoire et al., 2023: https://doi.org/10.25326/440). Any questions concerning this current database or the scheduled SPIRIT aircraft measurements in the future are welcomed by contacting the corresponding author.

Furthermore, there are also CO measurements on aircraft and balloon platforms referenced in AERIS database (https://www.aeris-data.fr/en/catalogue-en/), such as in-situ measurements during StraPolÉté in 2009 (Krysztofiak et al., 2012) and off-line AirCore measurements in 2017 (Hooghiem et al., 2020).

5 Code Availability

The 3D aircraft trajectories were plotted by OriginPro 2021 (https://www.originlab.com/, last access: ~~18 February~~July 18, 2023, license needed) and the background maps were inputted by a build-in application (Google Map Import, created by the OriginLab Technical Support, available at https://www.originlab.com/fileExchange/details.aspx?fid=344, last access: ~~18 February~~July 18, 2023).

6 Summary and Conclusion~~s~~

Thanks to the development of the ~~airborne~~ SPIRIT instrument, accurate airborne CO measurements (0.3 ppbv precision at 1σ and overall uncertainty < 4 ppbv) were achieved during the past decade (2011 – 2021). This database describes all aircraft CO measurements by SPIRIT during this period. More than 200 h of airborne measurements were conducted in Europe, South Asia, and West Africa. The measurement domain covers a wide area, including tropical, northern mid-latitude, and northern high-latitude regions. This database also includes two unique intercontinental measurements, one from Germany to Ghana via the West African coast, and the other one from Germany to Malaysia.

Generally, surface CO levels in Southern Asia, Europe, and the whole Mediterranean region Basin are at a similar level, namely with mixing ratios < 150 ppbv, which is lower than that the coastal region of West Africa (200-300 ppbv). Moreover, CO levels decrease with altitude for most measurements except at high latitude regions where CO increases with altitude. This database can be of particular interest for studying anthropogenic emissions (DACCIWA-2016), aviation emissions (TC2-2013), wildfire emissions (SHIVA-2011, DACCIWA-2016), shipping and offshore oil rig emissions (GLAM-2014, DACCIWA-2016), convective plumes (SHIVA-2011), urban background (ChemCalInt-2014, MAGIC-2019), and long-distance transport (GLAM-2014, MAGIC-2021). This database helps to understand such events and to constrain and improve relevant model approaches. For instance, based on SHIVA data, it is found that the convective system can significantly affect the composition of the upper troposphere (Krysztofiak et al., 2018; Hamer et al., 2021). Siberia forest fire could affect the atmosphere over the Mediterranean Basin through long-distance transport, which has been confirmed by measurements during the GLAM-2014 project with a combination of a trajectory model and a chemistry-transport model (Brocchi et al., 2018). Brocchi et al. (2019) analyzed DACCIWA measurements and found that offshore oil rigs could contribute to deteriorating the air quality in coastal regions of West Africa. Moreover, with the emerging utilization of satellite images, the importance of calibration of those measurements at a regional and/or a global scale becomes more and more significant, revealing the importance of the SPIRIT database. For example, CO measurements during the DACCIWA-2016 project will be used to validate satellite product from Measurement of Pollution in the Troposphere (MOPITT).

7 Author Contribution

C.X., G.K., and V.C. lead this study. All authors participated in- the development, data acquisition, and/or maintenance of SPIRIT during at least one field campaign. All authors commented on and approved this manuscript.

8 Competing Interests

The authors declare that they have no competing financial interests.

9 Acknowledgments

We are grateful to the LPC2E colleagues Gilles Chalumeau, Thierry Vincent, Kevin Le Letty, Olivier Chevillon, and Anne-Laure Pelé for the mechanical, electronic, ~~and ~~optical development~~-~~and aircraft campaign support and data analysis of the SPIRIT instrument, and the Master students Guillaume Robelet and Abdelmalek Bakha (University of Orléans) for their help with the data retrieval and visualization. We thank Hans Schlager (DLR) for facilitating access to SHIVA and DACCIWA projects and the associated DLR Falcon-20 aircraft. We thank SAFIRE (CNRS, Météo-France, CNES) for flying research aircraft in excellent conditions.

Funding: ~~Besides the projects listed in the main text, t~~This work was supported by the PIVOTS project provided by the Region Centre − Val de Loire (ARD 2020 program and CPER 2015 − 2020) and the Labex VOLTAIRE project (ANR-10-LABX-100-01, managed by the University of Orléans). Funding also came from the projects SHIVA (226224-FP7-ENV-2008-1), EUFAR2 TransNational Access, DACCIWA (Grant Agreement N°603502), ChArMEx-MISTRALS, ChemCalInt French initiative and MAGIC (CNRS-INSU, CNES, ADEME, Météo-France, CEA).~~7~~

10 References

Acharja, P., Ali, K., Trivedi, D. K., Safai, P. D., Ghude, S., Prabhakaran, T., and Rajeevan, M.: Characterization of atmospheric trace gases and water soluble inorganic chemical ions of PM_1 and $PM_{2.5}$ at Indira Gandhi International Airport, New Delhi during 2017–18 winter, Sci. Total Environ., 729, 138800, https://doi.org/10.1016/j.scitotenv.2020.138800, 2020.

Andreae, M. O., Acevedo, O. C., Araùjo, A., Artaxo, P., Barbosa, C. G. G., Barbosa, H. M. J., Brito, J., Carbone, S., Chi, X., Cintra, B. B. L., Da Silva, N. F., Dias, N. L., Dias-Júnior, C. Q., Ditas, F., Ditz, R., Godoi, A. F. L., Godoi, R. H. M., Heimann, M., Hoffmann, T., Kesselmeier, J., Könemann, T., Krüger, M. L., Lavric, J. V., Manzi, A. O., Lopes, A. P., Martins, D. L., Mikhailov, E. F., Moran-Zuloaga, D., Nelson, B. W., Nölscher, A. C., Santos Nogueira, D., Piedade, M. T. F., Pöhlker, C., Pöschl, U., Quesada, C. A., Rizzo, L. V., Ro, C. U., Ruckteschler, N., Sá, L. D. A., De Oliveira Sá, M., Sales, C. B., Dos Santos, R. M. N., Saturno, J., Schöngart, J., Sörgel, M., De Souza, C. M., De Souza, R. A. F., Su, H., Targhetta, N., Tóta, J., Trebs, I., Trumbore, S., Van Eijck, A., Walter, D., Wang, Z., Weber, B., Williams, J., Winderlich, J., Wittmann, F., Wolff, S., and Yáñez-Serrano, A. M.: The Amazon Tall Tower Observatory (ATTO): Overview of pilot measurements on ecosystem ecology, meteorology, trace gases, and aerosols, Atmos. Chem. Phys., 15, 10723–10776, https://doi.org/10.5194/acp-15-10723-2015, 2015.

Andrés Hernández, M. D., Hilboll, A., Ziereis, H., Förster, E., Krüger, O., Kaiser, K., Schneider, J., Barnaba, F., Vrekoussis, M., Schmidt, J., Huntrieser, H., Blechschmidt, A.-M., George, M., Nenakhov, V., Klausner, T., Holanda, B., Wolf, J., Eirenschmalz, L., Krebsbach, M., Pöhlker, M., Hedegaard, A., Mei, L., Pfeilsticker, K., Liu, Y., Koppmann, R., Schlager, H., Bohn, B., Schumann, U., Richter, A., Schreiner, B., Sauer, D., Baumann, R., Mertens, M., Jöckel, P., Kilian, M., Stratmann, G., Pöhlker, C., Campanelli, M., Pandolfi, M., Sicard, M., Gomez-Amo, J., Pujadas, M., Bigge, K., Kluge, F., Schwarz, A., Daskalakis, N., Walter, D., Zahn, A., Pöschl, U., Bönisch, H., Borrmann, S., Platt, U., and Burrows, J. P.: Overview: On the transport and transformation of pollutants in the outflow of major population centres – observational data from the EMeRGe European intensive operational period in summer 2017, Atmos. Chem. Phys. Discuss., 1–81, 2021.

Bourgeois, I., Peischl, J., Neuman, J. A., Brown, S. S., Allen, H. M., Campuzano-Jost, P., Coggon, M. M., DiGangi, J. P., Diskin, G. S., Gilman, J. B., Gkatzelis, G. I., Guo, H., Halliday, H. A., Hanisco, T. F., Holmes, C. D., Huey, L. G., Jimenez, J. L., Lamplugh, A. D., Lee, Y. R., Lindaas, J., Moore, R. H., Nault, B. A., Nowak, J. B., Pagonis, D., Rickly, P. S., Robinson, M. A., Rollins, A. W., Selimovic, V., St. Clair, J. M., Tanner, D., Vasquez, K. T., Veres, P. R., Warneke, C., Wennberg, P. O., Washenfelder, R. A., Wiggins, E. B., Womack, C. C., Xu, L., Zarzana, K. J., and Ryerson, T. B.: Comparison of airborne measurements of NO, NO2 , HONO, NOy , and CO during FIREX-AQ, Atmos. Meas. Tech., 15, 4901–4930, https://doi.org/10.5194/amt-15-4901-2022, 2022.

Brocchi, V., Krysztofiak, G., Catoire, V., Guth, J., Marécal, V., Zbinden, R., El Amraoui, L., Dulac, F., and Ricaud, P.: Intercontinental transport of biomass burning pollutants over the Mediterranean Basin during the summer 2014 ChArMEx-GLAM airborne campaign, Atmos. Chem. Phys., 18, 6887–6906, https://doi.org/10.5194/acp-18-6887-2018, 2018.

Brocchi, V., Krysztofiak, G., Deroubaix, A., Stratmann, G., Sauer, D., Schlager, H., Deetz, K., Dayma, G., Robert, C., Chevrier, S., and Catoire, V.: Local air pollution from oil rig emissions observed during the airborne DACCIWA campaign, Atmos. Chem. Phys., 19, 11401–11411, https://doi.org/10.5194/acp-19-11401-2019, 2019.

Brown, S. S., Thornton, J. A., Keene, W. C., Pszenny, A. A. P., Sive, B. C., Dubé, W. P., Wagner, N. L., Young, C. J., Riedel, T. P., Roberts, J. M., Vandenboer, T. C., Bahreini, R., Öztürk, F., Middlebrook, A. M., Kim, S., Hübler, G., and Wolfe, D. E.: Nitrogen, Aerosol Composition, and Halogens on a Tall Tower (NACHTT): Overview of a wintertime air chemistry field study in the front range urban corridor of Colorado, J. Geophys. Res. Atmos., 118, 8067–8085, https://doi.org/10.1002/jgrd.50537, 2013.

Catoire, V., Robert, C., Chartier, M., Jacquet, P., Guimbaud, C., and Krysztofiak, G.: The SPIRIT airborne instrument: a three-channel infrared absorption spectrometer with quantum cascade lasers for in situ atmospheric trace-gas measurements, Appl. Phys. B, 123, 244, https://doi.org/10.1007/s00340-017-6820-x, 2017.

Catoire, V., Krysztofiak, G., and Xue, C.: CO measured by SPIRIT during airborne campaigns, [Dataset]. Aeris, https://doi.org/10.25326/440, 2023.

Crawford, J. H., Ahn, J. Y., Al-Saadi, J., Chang, L., Emmons, L. K., Kim, J., Lee, G., Park, J. H., Park, R. J., Woo, J. H., Song, C. K., Hong, J. H., Hong, Y. D., Lefer, B. L., Lee, M., Lee, T., Kim, S., Min, K. E., Yum, S. S., Shin, H. J., Kim, Y. W., Choi, J. S., Park, J. S., Szykman, J. J., Long, R. W., Jordan, C. E., Simpson, I. J., Fried, A., Dibb, J. E., Cho, S. Y., and Kim, Y. P.: The Korea-United States air quality (KORUS-AQ) field study, Elementa, 9, 1–27, https://doi.org/10.1525/elementa.2020.00163, 2021.

Daellenbach, K. R., Uzu, G., Jiang, J., Cassagnes, L., Leni, Z., Vlachou, A., Stefenelli, G., Canonaco, F., Weber, S., Segers, A., Kuenen, J. J. P., Schaap, M., Favez, O., Albinet, A., Aksoyoglu, S., Dommen, J., Baltensperger, U., Geiser, M., El Haddad, I., Jaffrezo, J., and Prévôt, A. S. H.: Sources of particulate-matter air pollution and its oxidative potential in Europe, Nature, 587, 414–419, https://doi.org/10.1038/s41586-020-2902-8, 2020.

David, L. M., Ravishankara, A. R., Brey, S. J., Fischer, E. V, Volckens, J., and Kreidenweis, S.: Could the exception become the rule?

"Uncontrollable" air pollution events in the U.S. due to wildland fires, Environ. Res. Lett., 16, 034029, https://doi.org/10.1088/1748-9326/abe1f3, 2021.

Dekker, I. N., Houweling, S., Pandey, S., Krol, M., Röckmann, T., Borsdorff, T., Landgraf, J., and Aben, I.: What caused the extreme CO concentrations during the 2017 high-pollution episode in India?, Atmos. Chem. Phys., 19, 3433–3445, https://doi.org/10.5194/acp-19-3433-2019, 2019.

Fast, J. D., De Foy, B., Rosas, F. A., Caetano, E., Carmichael, G., Emmons, L., McKenna, D., Mena, M., Skamarock, W., Tie, X., Coulter, R. L., Barnard, J. C., Wiedinmyer, C., and Madronich, S.: A meteorological overview of the MILAGRO field campaigns, Atmos. Chem. Phys., 7, 2233–2257, https://doi.org/10.5194/acp-7-2233-2007, 2007.

Fehsenfeld, F. C., Ancellet, G., Bates, T. S., Goldstein, A. H., Hardesty, R. M., Honrath, R., Law, K. S., Lewis, A. C., Leaitch, R., McKeen, S., Meagher, J., Parrish, D. D., Pszenny, A. A. P., Russell, P. B., Schlager, H., Seinfeld, J., Talbot, R., and Zbinden, R.: International Consortium for Atmospheric Research on Transport and Transformation (ICARTT): North America to Europe - Overview of the 2004 summer field study, J. Geophys. Res. Atmos., 111, https://doi.org/10.1029/2006JD007829, 2006.

Formenti, P., D'Anna, B., Flamant, C., Mallet, M., Piketh, S. J., Schepanski, K., Waquet, F., Auriol, F., Brogniez, G., Burnet, F., Chaboureau, J. P., Chauvigné, A., Chazette, P., Denjean, C., Desboeufs, K., Doussin, J. F., Elguindi, N., Feuerstein, S., Gaetani, M., Giorio, C., Klopper, D., Mallet, M. D., Nabat, P., Monod, A., Solmon, F., Namwoonde, A., Chikwililwa, C., Mushi, R., Welton, E. J., and Holben, B.: The aerosols, radiation and clouds in southern Africa field campaign in Namibia overview, illustrative observations, and way forward, Bull. Am. Meteorol. Soc., 100, 1277–1298, https://doi.org/10.1175/BAMS-D-17-0278.1, 2019.

Forster, E., Bonisch, H., Neumaier, M., Obersteiner, F., Zahn, A., Hilboll, A., Kalisz Hedegaard, A. B., Daskalakis, N., Poulidis, A. P., Vrekoussis, M., Lichtenstern, M., and Braesicke, P.: Chemical and dynamical identification of emission outflows during the HALO campaign EMeRGe in Europe and Asia, Atmos. Chem. Phys., 23, 1893–1918, https://doi.org/10.5194/acp-23-1893-2023, 2023.

Gratton, G. B.: The Meteorological Research Flight and its predecessors and successors, J. Aeronaut. Hist., 6, 2012.

Guo, S., Hu, M., Zamora, M. L., Peng, J., Shang, D., Zheng, J., Du, Z., Wu, Z., Shao, M., Zeng, L., Molina, M. J., and Zhang, R.: Elucidating severe urban haze formation in China, Proc. Natl. Acad. Sci., 111, 17373–17378, https://doi.org/10.1073/pnas.1419604111, 2014.

Hahn, V., Meerkötter, R., Voigt, C., Gisinger, S., Sauer, D., Catoire, V., Dreiling, V., Coe, H., Flamant, C., Kaufmann, S., Kleine, J., Knippertz, P., Moser, M., Rosenberg, P., Schlager, H., Schwarzenboeck, A., and Taylor, J.: Pollution slightly enhances atmospheric cooling by low-level clouds in tropical West Africa, Atmos. Chem. Phys. Discuss., 2022, 1–21, https://doi.org/10.5194/acp-2022-795, 2022.

Hamburger, T., McMeeking, G., Minikin, A., Birmili, W., Dall'Osto, M., O'Dowd, C., Flentje, H., Henzing, B., Junninen, H., Kristensson, A., De Leeuw, G., Stohl, A., Burkhart, J. F., Coe, H., Krejci, R., and Petzold, A.: Overview of the synoptic and pollution situation over Europe during the EUCAARI-LONGREX field campaign, Atmos. Chem. Phys., 11, 1065–1082, https://doi.org/10.5194/acp-11-1065-2011, 2011.

Hamer, P. D., Marecal, V., Hossaini, R., Pirre, M., Krysztofiak, G., Ziska, F., Engel, A., Sala, S., Keber, T., Bonisch, H., Atlas, E., Kruger, K., Chipperfield, M., Catoire, V., Samah, A. A., Dorf, M., Siew Moi, P., Schlager, H., and Pfeilsticker, K.: Cloud-scale modelling of the impact of deep convection on the fate of oceanic bromoform in the troposphere: A case study over the west coast of Borneo, Atmos. Chem. Phys., 21, 16955–16984, https://doi.org/10.5194/acp-21-16955-2021, 2021.

Hanke, M., Umann, B., Uecker, J., Arnold, F., and Bunz, H.: Atmospheric measurements of gas-phase HNO3 and SO2 using chemical ionization mass spectrometry during the MINATROC field campaign 2000 on Monte Cimone, Atmos. Chem. Phys., 3, 417–436, https://doi.org/10.5194/acp-3-417-2003, 2003.

Harrison, R. M., Dall'Osto, M., Beddows, D. C. S., Thorpe, A. J., Bloss, W. J., Allan, J. D., Coe, H., Dorsey, J. R., Gallagher, M., Martin, C., Whitehead, J., Williams, P. I., Jones, R. L., Langridge, J. M., Benton, A. K., Ball, S. M., Langford, B., Hewitt, C. N., Davison, B., Martin, D., Petersson, K. F., Henshaw, S. J., White, I. R., Shallcross, D. E., Barlow, J. F., Dunbar, T., Davies, F., Nemitz, E., Phillips, G. J., Helfter, C., Di Marco, C. F., and Smith, S.: Atmospheric chemistry and physics in the atmosphere of a developed megacity (London): An overview of the REPARTEE experiment and its conclusions, Atmos. Chem. Phys., 12, 3065–3114, https://doi.org/10.5194/acp-12-3065-2012, 2012.

Haywood, J. M., Abel, S. J., Barrett, P. A., Bellouin, N., Blyth, A., Bower, K. N., Brooks, M., Carslaw, K., Che, H., Coe, H., Cotterell, M.

I., Crawford, I., Cui, Z., Davies, N., Dingley, B., Field, P., Formenti, P., Gordon, H., De Graaf, M., Herbert, R., Johnson, B., Jones, A. C., Langridge, J. M., Malavelle, F., Partridge, D. G., Peers, F., Redemann, J., Stier, P., Szpek, K., Taylor, J. W., Watson-Parris, D., Wood, R., Wu, H., and Zuidema, P.: The CLoud-Aerosol-Radiation Interaction and Forcing: Year 2017 (CLARIFY-2017) measurement campaign, Atmos. Chem. Phys., 21, 1049–1084, https://doi.org/10.5194/acp-21-1049-2021, 2021.

Hegarty, J. D., Cady-Pereira, K. E., Payne, V. H., Kulawik, S. S., Worden, J. R., Kantchev, V., Worden, H. M., McKain, K., Pittman, J. V, Commane, R., Daube Jr., B. C., and Kort, E. A.: Validation and error estimation of AIRS MUSES CO profiles with HIPPO, ATom, and NOAA GML aircraft observations, Atmos. Meas. Tech., 15, 205–223, https://doi.org/10.5194/amt-15-205-2022, 2022.

Hooghiem, J. J. D., Popa, M. E., Röckmann, T., Grooß, J.-U., Tritscher, I., Müller, R., Kivi, R., and Chen, H.: Wildfire smoke in the lower stratosphere identified by in situ CO observations, Atmos. Chem. Phys., 20, 13985–14003, https://doi.org/10.5194/acp-20-13985-2020, 2020.

Jaffe, D., Schnieder, B., and Inouye, D.: Technical note: Use of $PM_{2.5}$ to CO ratio as a tracer of wildfire smoke in urban areas, Atmos. Chem. Phys. Discuss., 2022, 1–15, https://doi.org/10.5194/acp-2022-138, 2022.

Jaffe, D. A. and Wigder, N. L.: Ozone production from wildfires: A critical review, Atmos. Environ., 51, 1–10, https://doi.org/10.1016/j.atmosenv.2011.11.063, 2012.

Johnson, B. T., Osborne, S. R., Haywood, J. M., and Harrison, M. A. J.: Aircraft measurements of biomass burning aerosol over West Africa during DABEX, J. Geophys. Res. Atmos., 113, 1–15, https://doi.org/10.1029/2007JD009451, 2008.

Kniffka, A., Knippertz, P., and Fink, A. H.: The role of low-level clouds in the West African monsoon system, Atmos. Chem. Phys., 19, 1623–1647, https://doi.org/10.5194/acp-19-1623-2019, 2019.

Knippertz, P., Coe, H., Chiu, J. C., Evans, M. J., Fink, A. H., Kalthoff, N., Liousse, C., Mari, C., Allan, R. P., Brooks, B., Danour, S., Flamant, C., Jegede, O. O., Lohou, F., and Marsham, J. H.: The DACCIWA Project: Dynamics–Aerosol–Chemistry–Cloud Interactions in West Africa, Bull. Am. Meteorol. Soc., 96, 1451–1460, https://doi.org/10.1175/BAMS-D-14-00108.1, 2015.

Krysztofiak, G., Thiéblemont, R., Huret, N., Catoire, V., Té, Y., Jégou, F., Coheur, P. F., Clerbaux, C., Payan, S., Drouin, M. A., Robert, C., Jeseck, P., Attié, J. L., and Camy-Peyret, C.: Detection in the summer polar stratosphere of pollution plume from East Asia and North America by balloon-borne in situ CO measurements, Atmos. Chem. Phys., 12, 11889–11906, https://doi.org/10.5194/acp-12-11889-2012, 2012.

Krysztofiak, G., Catoire, V., Hamer, P. D., Marécal, V., Robert, C., Engel, A., Bönisch, H., Grossmann, K., Quack, B., Atlas, E., and Pfeilsticker, K.: Evidence of convective transport in tropical West Pacific region during SHIVA experiment, Atmos. Sci. Lett., 19, 1–7, https://doi.org/10.1002/asl.798, 2018.

Lelieveld, J., Butler, T. M., Crowley, J. N., Dillon, T. J., Fischer, H., Ganzeveld, L., Harder, H., Lawrence, M. G., Martinez, M., Taraborrelli, D., and Williams, J.: Atmospheric oxidation capacity sustained by a tropical forest, Nature, 452, 737–740, https://doi.org/10.1038/nature06870, 2008.

Luo, M., Rinsland, C., Fisher, B., Sachse, G., Diskin, G., Logan, J., Worden, H., Kulawik, S., Osterman, G., Eldering, A., Herman, R., and Shephard, M.: TES carbon monoxide validation with DACOM aircraft measurements during INTEX-B 2006, J. Geophys. Res. Atmos., 112, https://doi.org/10.1029/2007JD008803, 2007.

Machado, L. A. T., Calheiros, A. J. P., Biscaro, T., Giangrande, S., Silva Dias, M. A. F., Cecchini, M. A., Albrecht, R., Andreae, M. O., Araujo, W. F., Artaxo, P., Borrmann, S., Braga, R., Burleyson, C., Eichholz, C. W., Fan, J., Feng, Z., Fisch, G. F., Jensen, M. P., Martin, S. T., Pöschl, U., Pöhlker, C., Pöhlker, M. L., Ribaud, J.-F., Rosenfeld, D., Saraiva, J. M. B., Schumacher, C., Thalman, R., Walter, D., and Wendisch, M.: Overview: Precipitation characteristics and sensitivities to environmental conditions during GoAmazon2014/5 and ACRIDICON-CHUVA, Atmos. Chem. Phys., 18, 6461–6482, https://doi.org/10.5194/acp-18-6461-2018, 2018.

Mallet, M., Dulac, F., Formenti, P., Nabat, P., Sciare, J., Roberts, G., Pelon, J., Ancellet, G., Tanré, D., Parol, F., Denjean, C., Brogniez, G., di Sarra, A., Alados-Arboledas, L., Arndt, J., Auriol, F., Blarel, L., Bourrianne, T., Chazette, P., Chevaillier, S., Claeys, M., D'Anna, B., Derimian, Y., Desboeufs, K., Di Iorio, T., Doussin, J.-F., Durand, P., Féron, A., Freney, E., Gaimoz, C., Goloub, P., Gómez-Amo, J. L., Granados-Muñoz, M. J., Grand, N., Hamonou, E., Jankowiak, I., Jeannot, M., Léon, J.-F., Maillé, M., Mailler, S., Meloni, D., Menut, L., Momboisse, G., Nicolas, J., Podvin, T., Pont, V., Rea, G., Renard, J.-B., Roblou, L., Schepanski, K., Schwarzenboeck, A., Sellegri, K., Sicard, M., Solmon, F., Somot, S., Torres, B., Totems, J., Triquet, S., Verdier, N., Verwaerde, C., Waquet, F., Wenger, J., and Zapf, P.: Overview of the Chemistry-Aerosol Mediterranean Experiment/Aerosol Direct Radiative Forcing on the Mediterranean Climate (ChArMEx/ADRIMED) summer 2013 campaign, Atmos. Chem. Phys., 16, 455–504, https://doi.org/10.5194/acp-16-455-2016, 2016.

McMeeking, G. R., Hamburger, T., Liu, D., Flynn, M., Morgan, W. T., Northway, M., Highwood, E. J., Krejci, R., Allan, J. D., Minikin, A., and Coe, H.: Black carbon measurements in the boundary layer over western and northern Europe, Atmos. Chem. Phys., 10, 9393–9414, https://doi.org/10.5194/acp-10-9393-2010, 2010.

Palmer, P. I., Jacob, D. J., Jones, D. B. A., Heald, C. L., Yantosca, R. M., Logan, J. A., Sachse, G. W., and Streets, D. G.: Inverting for emissions of carbon monoxide from Asia using aircraft observations over the western Pacific, J. Geophys. Res. Atmos., 108, https://doi.org/10.1029/2003JD003397, 2003.

Permar, W., Wang, Q., Selimovic, V., Wielgasz, C., Yokelson, R. J., Hornbrook, R. S., Hills, A. J., Apel, E. C., Ku, I. T., Zhou, Y., Sive, B. C., Sullivan, A. P., Collett, J. L., Campos, T. L., Palm, B. B., Peng, Q., Thornton, J. A., Garofalo, L. A., Farmer, D. K., Kreidenweis, S. M., Levin, E. J. T., DeMott, P. J., Flocke, F., Fischer, E. V., and Hu, L.: Emissions of Trace Organic Gases From Western U.S. Wildfires Based on WE-CAN Aircraft Measurements, J. Geophys. Res. Atmos., 126, 1–29, https://doi.org/10.1029/2020JD033838, 2021.

Ravi Kant Pathak, Wai Shing Wu, and Tao Wang: Summertime $PM_{2.5}$ ionic species in four major cities of China: nitrate formation in an ammonia-deficient atmosphere, Atmos. Chem. Phys., 9, 1711–1722, https://doi.org/10.5194/acpd-8-11487-2008, 2009.

Redemann, J., Wood, R., Zuidema, P., Doherty, S. J., Luna, B., LeBlanc, S. E., Diamond, M. S., Shinozuka, Y., Chang, I. Y., Ueyama, R., Pfister, L., Ryoo, J. M., Dobracki, A. N., da Silva, A. M., Longo, K. M., Kacenelenbogen, M. S., Flynn, C. J., Pistone, K., Knox, N. M., Piketh, S. J., Haywood, J. M., Formenti, P., Mallet, M., Stier, P., Ackerman, A. S., Bauer, S. E., Fridlind, A. M., Carmichael, G. R., Saide, P. E., Ferrada, G. A., Howell, S. G., Freitag, S., Cairns, B., Holben, B. N., Knobelspiesse, K. D., Tanelli, S., L'Ecuyer, T. S., Dzambo, A. M., Sy, O. O., McFarquhar, G. M., Poellot, M. R., Gupta, S., O'Brien, J. R., Nenes, A., Kacarab, M., Wong, J. P. S., Small-Griswold, J. D., Thornhill, K. L., Noone, D., Podolske, J. R., Sebastian Schmidt, K., Pilewskie, P., Chen, H., Cochrane, S. P., Sedlacek, A. J., Lang, T. J., Stith, E., Segal-Rozenhaimer, M., Ferrare, R. A., Burton, S. P., Hostetler, C. A., Diner, D. J., Seidel, F. C., Platnick, S. E., Myers, J. S., Meyer, K. G., Spangenberg, D. A., Maring, H., and Gao, L.: An overview of the ORACLES (ObseRvations of aerosols above CLouds and their intEractionS) project: Aerosol-cloud-radiation interactions in the southeast Atlantic basin, Atmos. Chem. Phys., 21, 1507–1563, https://doi.org/10.5194/acp-21-1507-2021, 2021.

Ricaud, P., Zbinden, R., Catoire, V., Brocchi, V., Dulac, F., Hamonou, E., Canonici, J. C., El Amraoui, L., Massart, S., Piguet, B., Dayan, U., Nabat, P., Sciare, J., Ramonet, M., Delmotte, M., Di Sarra, A., Sferlazzo, D., Di Iorio, T., Piacentino, S., Cristofanelli, P., Mihalopoulos, N., Kouvarakis, G., Pikridas, M., Savvides, C., Mamouri, R. E., Nisantzi, A., Hadjimitsis, D., Attié, J. L., Ferré, H., Kangah, Y., Jaidan, N., Guth, J., Jacquet, P., Chevrier, S., Robert, C., Bourdon, A., Bourdinot, J. F., Etienne, J. C., Krysztofiak, G., and Theron, P.: The GLAM airborne campaign across the Mediterranean Basin, Bull. Am. Meteorol. Soc., 99, 361–380, https://doi.org/10.1175/BAMS-D-16-0226.1, 2018.

Ryerson, T. B., Andrews, A. E., Angevine, W. M., Bates, T. S., Brock, C. A., Cairns, B., Cohen, R. C., Cooper, O. R., De Gouw, J. A., Fehsenfeld, F. C., Ferrare, R. A., Fischer, M. L., Flagan, R. C., Goldstein, A. H., Hair, J. W., Hardesty, R. M., Hostetler, C. A., Jimenez, J. L., Langford, A. O., McCauley, E., McKeen, S. A., Molina, L. T., Nenes, A., Oltmans, S. J., Parrish, D. D., Pederson, J. R., Pierce, R. B., Prather, K., Quinn, P. K., Seinfeld, J. H., Senff, C. J., Sorooshian, A., Stutz, J., Surratt, J. D., Trainer, M., Volkamer, R., Williams, E. J., and Wofsy, S. C.: The 2010 California Research at the Nexus of Air Quality and Climate Change (CalNex) field study, J. Geophys. Res. Atmos., 118, 5830–5866, https://doi.org/10.1002/jgrd.50331, 2013.

Sellers, P., Hall, F., Ranson, K. J., Margolis, H., Kelly, B., Baldocchi, D., den Hartog, G., Cihlar, J., Ryan, M. G., Goodison, B., Crill, P., Lettenmaier, D., and Wickland, D. E.: The Boreal Ecosystem–Atmosphere Study (BOREAS): An Overview and Early Results from the 1994 Field Year, Bull. Am. Meteorol. Soc., 76, 1549–1577, https://doi.org/10.1175/1520-0477(1995)076<1549:TBESAO>2.0.CO;2, 1995.

Shi, Z., Vu, T., Kotthaus, S., Harrison, R. M., Grimmond, S., Yue, S., Zhu, T., Lee, J., Han, Y., Demuzere, M., Dunmore, R. E., Ren, L., Liu, D., Wang, Y., Wild, O., Allan, J., Joe Acton, W., Barlow, J., Barratt, B., Beddows, D., Bloss, W. J., Calzolai, G., Carruthers, D., Carslaw, D. C., Chan, Q., Chatzidiakou, L., Chen, Y., Crilley, L., Coe, H., Dai, T., Doherty, R., Duan, F., Fu, P., Ge, B., Ge, M., Guan, D., Hamilton, J. F., He, K., Heal, M., Heard, D., Nicholas Hewitt, C., Hollaway, M., Hu, M., Ji, D., Jiang, X., Jones, R., Kalberer, M., Kelly, F. J., Kramer, L., Langford, B., Lin, C., Lewis, A. C., Li, J., Li, W., Liu, H., Liu, J., Loh, M., Lu, K., Lucarelli, F., Mann, G., McFiggans, G., Miller, M. R., Mills, G., Monk, P., Nemitz, E., O'Connor, F., Ouyang, B., Palmer, P. I., Percival, C., Popoola, O., Reeves, C., Rickard, A.

R., Shao, L., Shi, G., Spracklen, D., Stevenson, D., Sun, Y., Sun, Z., Tao, S., Tong, S., Wang, Q., Wang, W., Wang, X., Wang, X., Wang, Z., Wei, L., Whalley, L., Wu, X., Wu, Z., Xie, P., Yang, F., Zhang, Q., Zhang, Y., Zhang, Y., and Zheng, M.: Introduction to the special issue "in-depth study of air pollution sources and processes within Beijing and its surrounding region (APHH-Beijing)," Atmos. Chem. Phys., 19, 7519–7546, https://doi.org/10.5194/acp-19-7519-2019, 2019.

Spackman, J. R., Gao, R. S., Neff, W. D., Schwarz, J. P., Watts, L. A., Fahey, D. W., Holloway, J. S., Ryerson, T. B., Peischl, J., and Brock, C. A.: Aircraft observations of enhancement and depletion of black carbon mass in the springtime Arctic, Atmos. Chem. Phys., 10, 9667–9680, https://doi.org/10.5194/acp-10-9667-2010, 2010.

Tang, Y. S., Flechard, C. R., Dämmgen, U., Vidic, S., Djuricic, V., Mitosinkova, M., Uggerud, H. T., Sanz, M. J., Simmons, I., Dragosits, U., Nemitz, E., Twigg, M., van Dijk, N., Fauvel, Y., Sanz, F., Ferm, M., Perrino, C., Catrambone, M., Leaver, D., Braban, C. F., Cape, J. N., Heal, M. R., and Sutton, M. A.: Pan-European rural monitoring network shows dominance of NH_3 gas and NH_4NO_3 aerosol in inorganic atmospheric pollution load, Atmos. Chem. Phys., 21, 875–914, https://doi.org/10.5194/acp-21-875-2021, 2021.

Taylor, J. W., Haslett, S. L., Bower, K., Flynn, M., Crawford, I., Dorsey, J., Choularton, T., Connolly, P. J., Hahn, V., Voigt, C., Sauer, D., Dupuy, R., Brito, J., Schwarzenboeck, A., Bourriane, T., Denjean, C., Rosenberg, P., Flamant, C., Lee, J. D., Vaughan, A. R., Hill, P. G., Brooks, B., Catoire, V., Knippertz, P., and Coe, H.: Aerosol influences on low-level clouds in the West African monsoon, Atmos. Chem. Phys., 19, 8503–8522, https://doi.org/10.5194/acp-19-8503-2019, 2019.

Voigt, C., Lelieveld, J., Schlager, H., Schneider, J., Curtius, J., Meerkötter, R., Sauer, D., Bugliaro, L., Bohn, B., Crowley, J. N., Erbertseder, T., Groß, S., Hahn, V., Li, Q., Mertens, M., Pöhlker, M. L., Pozzer, A., Schumann, U., Tomsche, L., Williams, J., Zahn, A., Andreae, M., Borrmann, S., Bräuer, T., Dörich, R., Dörnbrack, A., Edtbauer, A., Ernle, L., Fischer, H., Giez, A., Granzin, M., Grewe, V., Harder, H., Heinritzi, M., Holanda, B. A., Jöckel, P., Kaiser, K., Krüger, O. O., Lucke, J., Marsing, A., Martin, A., Matthes, S., Pöhlker, C., Pöschl, U., Reifenberg, S., Ringsdorf, A., Scheibe, M., Tadic, I., Zauner-Wieczorek, M., Henke, R., and Rapp, M.: Cleaner Skies during the COVID-19 Lockdown, Bull. Am. Meteorol. Soc., 103, E1796–E1827, https://doi.org/10.1175/BAMS-D-21-0012.1, 2022.

Wizenberg, T., Strong, K., Walker, K., Lutsch, E., Borsdorff, T., and Landgraf, J.: Intercomparison of CO measurements from TROPOMI, ACE-FTS, and a high-Arctic ground-based Fourier transform spectrometer, Atmos. Meas. Tech., 14, 7707–7728, https://doi.org/10.5194/amt-14-7707-2021, 2021.

Wu, H., Taylor, J. W., Langridge, J. M., Yu, C., Allan, J. D., Szpek, K., Cotterell, M. I., Williams, P. I., Flynn, M., Barker, P., Fox, C., Allen, G., Lee, J., and Coe, H.: Rapid transformation of ambient absorbing aerosols from West African biomass burning, Atmos. Chem. Phys., 21, 9417–9440, https://doi.org/10.5194/acp-21-9417-2021, 2021.

Xue, C., Zhang, C., Ye, C., Liu, P., Catoire, V., Krysztofiak, G., Chen, H., Ren, Y., Zhao, X., Wang, J., Zhang, F., Zhang, C., Zhang, J., An, J., Wang, T., Chen, J., Kleffmann, J., Mellouki, A., and Mu, Y.: HONO Budget and Its Role in Nitrate Formation in the Rural North China Plain, Environ. Sci. Technol., 54, 11048–11057, https://doi.org/10.1021/acs.est.0c01832, 2020.